Accepted Manuscript

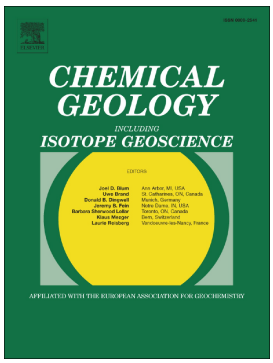

Influence of marine biochemical cycles on seasonal variation of Ba/Ca in the near-shore coral Cyphastrea, Rat Island, southern Great Barrier Reef

Narottam Saha, Gregory E. Webb, Jian-Xin Zhao, Nicole D. Leonard, Ai Duc Nguyen

PII: S0009-2541(18)30445-5
DOI: doi:10.1016/j.chemgeo.2018.09.005
Reference: CHEMGE 18898

To appear in: *Chemical Geology*

Received date: 23 November 2017
Revised date: 1 September 2018
Accepted date: 4 September 2018

Please cite this article as: Narottam Saha, Gregory E. Webb, Jian-Xin Zhao, Nicole D. Leonard, Ai Duc Nguyen , Influence of marine biochemical cycles on seasonal variation of Ba/Ca in the near-shore coral Cyphastrea, Rat Island, southern Great Barrier Reef. Chemge (2018), doi:10.1016/j.chemgeo.2018.09.005

Influence of marine biochemical cycles on seasonal variation of Ba/Ca in the near-shore coral *Cyphastrea*, Rat Island, southern Great Barrier Reef

Narottam Saha[1,2*], Gregory E. Webb[1], Jian-Xin Zhao[1], Nicole D. Leonard[1], Ai Duc Nguyen[1]

[1] School of Earth and Environmental Sciences, The University of Queensland, QLD 4072, Australia

[2] Centre for Mined Land Rehabilitation, Sustainable Mineral Institute, The University of Queensland, QLD 4072, Australia

Corresponding author: n.saha@uq.edu.au (N. Saha)

Abstract

Coral reef ecosystems maintain high biodiversity and have great economic value. Nonetheless, inshore coral reefs of the Great Barrier Reef (GBR) are facing threats from poor water quality due to extensive modification of coastal catchments following European settlement. Ba/Ca ratios in coral skeletons have been used to infer past water quality, but in order to use a proxy to infer past environments, it is critical to develop a firm understanding of the parameters that control the proxy. This study investigated various environmental, climatic and oceanographic factors to understand a long-term (1976 to 2016) record of biogeochemical cycling of Ba/Ca preserved in a *Cyphastrea* sp. coral colony recovered from near-shore Rat Island (near Port Curtis), southern GBR. Our *Cyphastrea* was found to have simple skeletal microstructure, similar to that of *Porites*, with unaltered skeletal preservation, clear annual density banding, and an extended growth history with seasonally resolved Sr/Ca signals. This combined with a wide geographic distribution make *Cyphastrea* coral a potential new palaeoenvironmental archive. Although Rat Island is located near the mainland and is influenced directly by discharge from the Calliope and Boyne rivers, temporal oscillations of Ba/Ca did not show peaks associated with high runoff during summers. Rather, Cyphastrea's high-resolution Ba/Ca data shows, for the first time, consistent seasonal cycles with a gradual decrease from spring through summer and gradual rise from autumn through winter. Biogeochemical cycling of Ba in the semi-confined turbid water of Port Curtis may be controlled by active or passive planktic uptake during the spring bloom stage and removal of barite minerals formed in decaying phytoplankton during post-bloom stage. The subsequent increase of Ba/Ca from autumn through winter may be attributed to reduction of phytoplankton abundance. The semi-enclosed embayment of Port Curtis has restricted water turnover with a large terrigenous runoff load that may have significant influence on phytoplankton dynamics. Our work suggests that Ba cycling, and hence, the Ba/Ca coral

proxy, may differ greatly depending on local geographic factors and thus, we recommend that geographic and oceanographic conditions should be taken into account in coral-based Ba/Ca proxy studies used to reconstruct water quality.

Keywords: Water quality, Ba/Ca, *Cyphastrea* sp., Phytoplankton, Great Barrier Reef.

1. Introduction

Coral reefs are threatened worldwide by changes in environmental and climate components from global (e.g., ocean acidification and global warming) (Hoegh-Guldberg et al., 2007) and local (e.g., poor water quality) (De'ath et al., 2012; Clark et al., 2017) pressures. Local anthropogenic activities, including intensive agricultural practices (Packett et al., 2009; Thorburn et al., 2013) and land use changes (Seabrook et al., 2006; Lewis et al., 2007; Seabrook et al., 2007; Hunter and Walton, 2008) with associated increased sediment runoff (Fabricius, 2005; Lough et al., 2015) are major threats to inshore coral reefs. Such reefs comprise one-third of the Great Barrier Reef (GBR) (Hopley et al., 2007). High sediment discharge in turn significantly affects key water quality parameters, such as water turbidity, total suspended solid load (Kroon et al., 2012), nutrient content (Wooldridge et al., 2006; Kroon et al., 2012) and primary productivity (Furnas et al., 2005; Brodie et al., 2007; Brodie et al., 2011; Schaffelke et al., 2012). Declining water quality hampers coral survival capacity (De'ath and Fabricius, 2010), reduces coral growth (Rogers, 1990; Carilli et al., 2009) and larval recruitment and settlement success (Rogers, 1990; Dikou and van Woesik, 2006; Erftemeijer et al., 2012), affects species composition (Pastorok and Bilyard, 1985; Dikou and van Woesik, 2006), reduces reef accretion rates (Rogers, 1990), enhances susceptibility to bleaching (Wagner et al., 2010; Cunning and Baker, 2013), affects coral colony forms (Fabricius and Wolanski, 2000; Weber et al., 2012), decreases photosynthesis, and disrupts coral-symbiont partnerships (Erftemeijer et al., 2012; Flores et al., 2012; Jones et al., 2016). Hence, proxy based reconstruction of water quality drivers (e.g., river discharge), especially to investigate pre-industrial water quality records, is important if we are to understand past responses of coral reefs to changes in water conditions and to project future responses under different anthropogenic scenarios.

Scleractinian corals secrete an aragonite ($CaCO_3$) skeleton throughout their growth and annually banded skeletons from massive corals are an invaluable archive of information in the form of palaeoenvironmental proxies (Gagan et al., 1998; McCulloch et al., 2003; Wyndham et al., 2004; Fleitmann et al., 2007; Kelly et al., 2009; DeLong et al., 2013). Water dissolved trace metals with ionic radii and charge similar to Ca can easily substitute for Ca in the aragonite crystal lattice in coral skeleton and therefore may represent the ambient water quality through its growing time. Among trace metal ratios used for monitoring fluvially derived sediments in coastal marine environments, Ba/Ca is the most widely used proxy (see review by Saha et al., 2016). Barium is incorporated into coral aragonite by substituting for Ca due to reasonable ionic size matching between divalent Ba (1.35 Å) and Ca (1.00 Å) (Shannon, 1976). Direct calibration of coralline Ba/Ca against seawater Ba/Ca has a distribution coefficient of ~1.0 (LaVigne et al., 2016), showing that Ba incorporates into coral in the same proportion as in ambient seawater. A primary source of Ba in the estuarine mixing zone is riverine input from continental weathering (Coffey et al., 1997). Once freshwater encounters more saline oceanic water with higher ionic strength, particle–bound Ba desorbs and is transported towards the ocean in river plumes (Hanor and Chan, 1977; Coffey et al., 1997). Desorption of particle-complexed Ba in coastal waters [~50–70% of total dissolved Ba (Li and Chan, 1979; Carroll et al., 1993)] is responsible for a clear contrast in Ba concentration between coastal and oceanic waters (Ba concentration in seawater ranges from 30 to 160 nM) (Wolgemuth and Broecker, 1970; Chan et al., 1976). Dissolved Ba in marine water shows depletion in the surface ocean and enrichment at depth (Jacquet et al., 2007; Hoppema et al., 2010). Because of its nutrient-like vertical concentration profile, which is closely linked to phytoplankton productivity (Dehairs et al., 1980), Ba/Ca in surface corals of offshore/oceanic settings has been used to reconstruct upwelling events (Lea et al., 1989; Reuer et al., 2003; Montaggioni et al., 2006). However, the complex biogeochemistry of Ba

in coastal coral skeletons is not fully understood, particularly in cases where multiple environmental and climatic drivers may interact simultaneously. Although skeletal Ba/Ca in some locations shows a correlation with regional river discharge (McCulloch et al., 2003; Fleitmann et al., 2007; Walther et al., 2013; Saha et al., 2018), anomalous Ba/Ca spikes uncorrelated with river discharge and/or any known event also are common (Sinclair, 2005b; Lewis et al., 2012; Saha et al., 2016; Saha et al., 2018). Hence, more spatiotemporal studies are needed to better understand the factors that control Ba/Ca dynamics in coral skeletons.

The majority of coral skeleton trace element studies from low to mid-latitude in the GBR are restricted to the species *Porites* (see review by Saha et al., 2016) owing to its higher abundance in tropical reefs and its long growth records with clear annual banding (Veron, 2000; McCulloch et al., 2003; Walther et al., 2013; Saha et al., 2018). However, although *Porites* is common in some inshore reefs of the GBR (Potts et al., 1985) it is currently absent or rare in many high-latitude inshore environments, such as sub-tropical Rat Island of southern GBR (Ayling et al., 2012) and Moreton Bay (Wallace et al., 2009). Hence, *Porites*-based palaeoenvironmental reconstructions are temporally and spatially limited and the investigation of alternative coral genera as palaeoenvironmental archives is warranted. Massive *Cyphastrea* sp. coral species are widely distributed in tropical and sub-tropical regions of the GBR (Veron, 2000). No previous study has exploited Ba/Ca records in the inshore coral *Cyphastrea* sp. to examine the biogeochemical cycles of Ba in coastal waters and coral-based Ba/Ca records are rare in reefs of the southern GBR with the exception of a recent publication based on *Porites* (Saha et al., 2018, also see their Fig. 1). No coral geochemical study has been conducted to infer long-term changes in water quality in the Gladstone region of the southern GBR. Here we report a 41-year, Ba/Ca record derived from inshore *Cyphastrea* sp. coral colonies from Rat Island (off Gladstone) to investigate the

influence of environmental, climatic, and oceanographic drivers on this widely used water quality proxy in an inshore turbid environment.

2. Materials and methods

2.1. Study area

Gladstone, located ~525 km north of Brisbane, is a major port city in Queensland, Australia. Port Curtis (also known as Port of Gladstone) is Queensland's largest multi-commodity port and the 4th largest coal export terminal in the world (GPC, 2014). Water in the embayment of Port Curtis (PC) is enclosed by Curtis Island (length ~44 km) on the north and Facing Island (length ~ 12 km) on the east and south-east sides. Three openings, including South Channel, North Channel and The Narrows, connect the water of PC to open ocean (Witt et al., 2009) (Fig. 1). Port Curtis contains a number of small islands, including Rat Island (present sampling site) located in the middle of the 'North Channel'. Rat Island is situated at a distance of ~10 km and ~18 km from the mouth of the Calliope and Boyne rivers, respectively. Fringing coral reefs occur on the rocky substrate adjacent to the Rat Island (Conaghan, 1966), although these reefs are poorly developed and show relatively low coral diversity.

The Calliope and Boyne rivers, which drain the hinterland near PC, influence the water quality of the PC estuary. The Boyne River delivers discharge to PC estuary via two channels—east (true mouth) and west (South Trees inlet) of Boyne Island (Fig. 1). Several smaller creeks also flow into the estuary from the mainland. Model-based estimation shows that current annual delivery of total suspended solids (TSS) to the GBR from the Calliope (~ 210 ktonnes/yr) and Boyne river (~ 43 ktonnes/yr) basins has increased by a factor of 10.5, and 1.0, respectively, compared to the period prior to European colonisation (Kroon et al., 2012). Similarly, current annual supply of total nitrogen (TN) and total phosphorous (TP)

increased by a factor of 13 (TN—from 46 to 600 tonnes/yr) and 26.7 (TP—from 6 to 160 tonnes/yr), respectively, from the Calliope River basin and by a factor of 2.1 (TN—from 90 to 190 tonnes/yr) and 2.1 (TP—from 14 to 30 tonnes/yr), respectively, from the Boyne River basin compared to pre-European settlement (Kroon et al., 2012). Apart from riverine delivery of terrestrial sediment, water quality in this region is influenced by numerous industries, agricultural activities, and dredging and dumping associated with Port development and operations (Petus and Devlin, 2012).

Climate of the region is characterized by a wet summer season (October to March) and dry a winter season (April to September). Summers are usually associated with considerable rainfall and higher relative humidity; winters are associated with minimal rainfall, relatively cooler temperature and lower humidity. Summer monsoonal rainfall shows substantial interannual to decadal variability (Kiem et al., 2003; Verdon et al., 2004). Variability of rainfall and river discharge is modulated by El Niño Southern Oscillation (ENSO) on an annual scale and Pacific Decadal Oscillation (PDO) on a decadal scale (Kiem et al., 2003; Kiem and Franks, 2004; Rodriguez-Ramirez et al., 2014). Occasional tropical cyclones developed in the Coral Sea bring torrential rain, storm surges, and high wave energy to the Queensland coast, typically during the summer season. South-east trade winds and Coriolis force drives freshwater plumes northward from the river mouths along the Queensland coast (King et al., 2001).

2.2. Coral sample collection and processing

In June 2016, two cores (core ID: RI1 and RI2) were extracted from two live *Cyphastrea* colonies from the same location using a pneumatic drill on SCUBA at 1.5 m below lowest astronomical tide (LAT) from a site (23.76631° S, 151.31778° E) on the southern side of Rat Island, located in the southern GBR (Fig. 1). The cores were washed with freshwater and

then cut longitudinally into ~ 7 mm thick slices using a diamond saw. Coral slabs were ultrasonically cleaned several times with Milli-Q water (18.2 Ω) and subsequently oven-dried at 60° C for 24 hrs. Dried coral slices were x-rayed to visualize annual density banding to aid sampling along the growth axis, chronology assignment and obtain information regarding annual extension rates. Annual linear extension rates for two cores were calculated from the linear distance between successive density couplets as the density bands for both the cores are clearly visible on X-radiographs (Fig. 2a,b). Mean annual linear extension rate was calculated by averaging the annual values. Coral slabs were then treated with 10% hydrogen peroxide (H_2O_2) for 48 hrs to eliminate organic contaminants and cleaned three times in an ultrasonic bath using Milli-Q water followed by drying in the oven at 60° C for 48 hrs. Sub-samples were manually milled from the dried slices along the growth axis using a drill (Dremel) equipped with a diamond bit of 2 mm diameter. Sequential sub-samples (8–12 per annual band) were then collected along the growth axis using a hand-held drill.

2.3. Elemental analysis and microstructure observation

Inductively Coupled Plasma-Mass Spectrometery (ICPMS–Thermo X-series II) was used to measure elements in coral skeleton at the Radiogenic Isotope Facility (RIF), The University of Queensland (UQ), Australia. All analytical containers, including bottles and test tubes, were cleaned in sub-boiling ~20% HNO_3 followed by Milli-Q water and then air-dried in HEPA-filtered hoods. Sample powders of ~1.5 mg were digested with 4.5 ml of 2% HNO_3 containing 6-ppb of ^{6}Li, ^{61}Ni, ^{103}Rh, ^{115}In, ^{187}Re and ^{235}U isotopes as internal standards, to achieve a final dilution factor of ~ 1: 3,500. Dilute solutions (~1:3,500) of certified geochemical reference materials W-2a (U.S.G.S. diabase standard), BHVO-2 (U.S.G.S. basalt standard), JCp-1 (Japanese coral), and BIR-1 (U.S.G.S. Icelandic basalt) were prepared from pre-made concentrated stock solutions. The final solutions of these standards also

contain the same 6ppb multi-isotope internal standards in 2% HNO_3. A mixture of JCp-1 and W2a solutions was also prepared to use as an external drift monitoring solution. The drift-monitoring solution was measured frequently (every five samples). Raw elemental signals were corrected for any mass response drift and matrix effects using the signal strengths of the multi-isotope internal standard, and then corrected for any long-term instrumental drift based on the signal variation of the repeatedly measured drift-monitoring solution. The mean JCp-1 values and standard deviations (n = 9) for Sr/Ca and Ba/Ca during the course of this study were 8.79 ± 0.04 (1 σ) mmol/mol and 7.46 ± 0.03 (1 σ) μmol/mol, respectively. Based on these analyses, the long-term reproducibility was calculated at 0.25% RSD for Sr/Ca and 0.46% RSD for Ba/Ca.

A scanning electron microscope (SEM–Hitachi TM3030Plus) was used on uncoated samples of the core to observe the skeletal microstructure and diagenetic preservation. Resin-impregnated samples (one longitudinal and one transverse section) were polished and etched using 2% formic acid for 20s prior to the observation.

2.4. Sources of environmental data

Monthly resolution sea surface temperature (SST) data were obtained from: (1) *in situ* SST data for the period of Oct 2013 to Sep 2015 from the Australian Institute of Marine Science (AIMS) Buoy at Masthead Reef (MASTHEADFL1; ~ 48 km east of Rat Island) at 1.5 m below LAT level (http://www.aims.gov.au/docs/data-centre/seatemperatures.html); (2) *in situ* SST data from Jun 2016 to Apr 2017 from the AIMS Buoy at Rat Island (RATFL1 at 2 m below LAT level); (3) satellite-derived SST data from IGOSS-NMC (https://iridl.ldeo.columbia.edu/SOURCES/.IGOSS/.nmc/.Reyn_SmithOIv2/.monthly/.sst/index.html?Set-Language=en) for the period of November 1981 to June 2016 and (4) Hadley Centre Global Sea Ice and Sea Surface Temperature (HadISST) dataset produced by Met

Office Hadley Centre (http://www.ceda.ac.uk/) from Jan 1976 to Jul 2015. The IGOSS-NMC and HadISST datasets were available for a 1° latitude by longitude box centered on 23.5°S, 151.5°E (off Rat Island). SST records from the three sources were highly correlated ($p < 0.01$) with linear regression coefficients, r^2 of 0.99 for AIMS (Masthead)–IGOSS, 0.97 for IGOSS–HadISST (supplementary Fig. S1). HadISST data from Jan 1976 to Oct 1981 and IGOSS SST data from Nov 1981 to Jun 2016 were combined and the composite SST was compared against Sr/Ca to develop coral chronology (discussed in section 2.5).

River discharge data (ML) were obtained from Department of Natural Resources and Mines (DNRM) Water Monitoring Information Portal (WMIP) gauging stations (https://water-monitoring.information.qld.gov.au/) on the Calliope River basin at Castlehope (station number 132001A). Rainfall data (mm) were sourced from the Australian Bureau of Meteorology (BOM—www.bom.gov.au) at Southern Curtis Island (station number 039241).

Monthly time series satellite-derived chlorophyll-a concentration data representing Sep 1997–Oct 2010 were obtained from the Sea Viewing Wide Field of View Sensor (SeaWiFS) via the NASA GES-DISC Interactive Online Visualization and ANalysis Infrastructure (GIOVANNI) web interface (https://giovanni.gsfc.nasa.gov/giovanni/). Data with 9 km spatial resolution were averaged for the regions of 23.8458°S and 151.2927°E, 23.7003°S and 151.4026°E. Daily resolution *in situ* total chlorophyll concentration data were sourced from Australian Institute of Marine Science (AIMS—http://data.aims.gov.au/metadataviewer/uuid/8a698de1-3fbf-48a5-b068-358b07aad35c) at Pelican Island (23.2389°S and 150.8745°E ; ~ 25 km north of Fitzroy River mouth) over the period of Oct 2007–Mar 2015. Monthly resolution *in situ* chlorophyll-a concentration data measured by Queensland Environmental Protection Agency (from 1995 to 2001) at Calliope River mouth and dissolved phosphate concentration data (1998-2001) measured by Gladstone Port Authority at Clinton Wharf were sourced from Currie and Small (2005). Solar exposure

data (monthly resolution from 1990 to 2015) were taken from BOM (http://www.bom.gov.au/climate/data/) at Southern Curtis Island (station number 039241). Daily wind speed data (1976 to 2015) recorded at Gladstone Radar (station number 039123) were obtained from BOM (http://www.bom.gov.au/climate/data/). The historical tide height dataset (2011-2014) for Auckland Point at Gladstone was sourced from Maritime Safety Queensland (https://www.msq.qld.gov.au/Tides/Open-data). Tropical cyclones that have been tracked within a 200 km radius of Rat Island from 1976 to 2006 were sourced from BOM (http://www.bom.gov.au/cgi-bin/silo/cyclones.cgi) and cyclonic history after 2006 was synthesised from other sources (http://www.australiasevereweather.com/cyclones/index.html; http://www.bom.gov.au/cyclone/history/; http://www.windworker.com.au/qldcyclones.htm) and listed in supplementary Table S1.

2.5. Coral chronology

Age models of the RI1 and RI2 cores were constructed by counting the annual density bands visible in the X-radiographs (Fig. 2). These visually developed chronologies were tested and refined by tuning the Sr/Ca data to monthly averaged SST since the inverse dependency of the coral Sr/Ca on ambient SST has been validated by many independent studies (Beck et al., 1992; Gagan et al., 1998; DeLong et al., 2011; DeLong et al., 2013; Bolton et al., 2014; Sadler et al., 2016). Thus, low winter SST corresponds to peak Sr/Ca and vice versa. After tuning the Sr/Ca peaks and troughs with monthly SST, geochemical data between the summer and winter tie-points were interpolated linearly to monthly resolution using the geochronological software AnalySeries 2.0 (Paillard et al., 1996) to facilitate comparisons between monthly instrumental datasets and monthly coral geochemical records.

2.6. Data analysis

Temporally uneven geochemical data (Sr/Ca and Ba/Ca) from each annual growth band were interpolated to evenly distributed monthly resolution data using AnalySeries 2.0 (Paillard et al., 1996) (see the 'Chronology' section above for detailed interpolation technique). Interpolated monthly data were used subsequently to perform continuous wavelet transform (CWT) to identify any periodicity. Cross wavelet transform (XWT) and wavelet coherence (WTC) were applied to analyse the relationships between two time series (SST–Ba/Ca and Sr/Ca–Ba/Ca) together in the time-frequency space. These wavelet analyses (CWT, XWT and WTC) were performed in Matlab using the software package (http://paos.colorado.edu/research/wavelets/) developed by Grinsted et al. (2004), which utilises the original continuous wavelet package of Torrence and Compo (1998).

3. Results

As *Cyphastrea* has not previously been used as a geochemical archive, the first issue was to investigate its microstructure and diagenetic preservation. The skeletal microstructure of *Cyphastrea* is similar to that of *Porites* (Nothdurft and Webb, 2007) consisting of aragonite fibres radiating from centers of rapid accretion (CRA) as trabeculae and then covered by thickening deposits (TD) consisting of more parallel aragonite fibres (Fig. 3). Skeletal architecture is simple with parallel vertically oriented corallites that are separated by coenosteum. Individual corallites consist of a circular wall (i.e., theca) and septa radiating towards the center of the corallite, both composed of vertically arranged parallel trabeculae (Fig.3). Dissepiments are scattered and there is no evidence of early marine diagenetic alteration (Fig. 3). Hence, considering the well-developed annual banding, the studied *Cyphastrea* colonies appear to be appropriate for geochemical analysis.

Development of an accurate chronology for geochemical time series is an important aspect of interpreting the modulation of proxies with environmental and climatic parameters.

Clear annual density bands that are visible in X-ray and distinguishable annual cycles of the commonly used SST proxy, Sr/Ca, in RI2 and RI1 cores allow us to develop a precise chronology for the *Cyphastrea* colonies. The time series for the interpolated Sr/Ca developed following the methods detailed in section 2.5 is shown in Fig. 2c,d. The geochemical records in the long RI2 record extend from Jun 2016 to Jan 1976 and in RI1 from Jul 2006 to Aug 2002. For RI1, a short unaltered portion with a ~4 year growth record was selected to cross-check the reproducibility of elemental ratios in RI2. The variability of unsmoothed RI2 Sr/Ca over the period of Jan 1976 to Jun 2016 ranged from 8.81 to 9.41 mmol/mol, with a mean value of 9.11 ± 0.11 (1σ) mmol/mol. Sr/Ca (unsmoothed from Aug 2002 to Jul 2006) in RI1 ranged from 9.07 to 9.57 mmol/mol with a mean value of 9.28 ± 0.11 (1σ) mmol/mol. The mean value of unsmoothed Sr/Ca in RI1 (9.28 ± 0.11 mmol/mol) over the common period (Aug 2002 to Jul 2006) is slightly higher than RI2 (varied from 9.07 to 9.57 mmol/mol with a mean of 9.17 ± 0.11 mmol/mol). The two Sr/Ca time series (smoothed) from Aug 2002 to Jul 2006 were significantly correlated (r = 0.68, n = 48, p < 0.01).

Annual linear extension rate in RI2 from 1976 to 2015 varied from 3.9 to 10.9 mm/yr with an average of 6.84 ± 1.5 (1σ) mm/yr, whereas annual linear extension rate in RI1 from 2003 to 2006 varied from 5.70 to 7.90 mm/yr with an average of 6.93 ± 0.93 (1σ) mm/yr, which is similar to the extension rate of RI2 (5.30 to 7.80 mm/yr with an average of 6.73 ± 1.05 (1σ) mm/yr) during the same overlapping period with significantly strong correlation (r = 0.71, n = 4, p < 0.01).

Unsmoothed Ba/Ca ratios in RI2 for the period of 1976 through 2016 varied from 4.26 to 13.93 µmol/mol with a mean value of 7.40 ± 2.05 (1σ) µmol/mol. The mean unsmoothed Ba/Ca values for cores RI1 and RI2 over the period of Aug 2002 to Jul 2006 were 6.67 ± 1.45 (1σ) µmol/mol and 6.03 ± 0.83 (1σ) µmol/mol, respectively. The range of Ba/Ca variability in RI2 (4.75 to 9.91 µmol/mol) was higher than for RI1 (4.91 to 7.99

μmol/mol) during the overlapping period (Aug 2002 to Jul 2006). The two Ba/Ca time series (smoothed) from Aug 2002 to Jul 2006 were significantly correlated (r = 0.42, n = 48, p < 0.01) with identical seasonal cycles (Fig. 4). The reported mean Ba/Ca for RI1 and RI2 and were significantly higher than the values registered in *Porites* from Round Top Island (Jupiter et al., 2008), Havannah Reef (McCulloch et al., 2003; Walther et al., 2013), Pandora Reef (McCulloch et al., 2003) and Great Keppel Island of the GBR (Saha et al., 2018) (Fig. 4). This likely reflects the naturally turbid environment of Port Curtis, possibly due to its semi-enclosure by Facing and Curtis islands, which form a significant circulation barrier between Port Curtis and the open ocean water (Fig. 1). Thus, the fresh water and terrestrial sediments discharged into this shallow embayment disperse slowly and poor water quality with higher turbidity may persist. Unlike, Great Keppel Island coral (Saha et al., 2018) and other reported studies (McCulloch et al., 2003; Jupiter et al., 2008; Walther et al., 2013) wherein Ba/Ca peaks seem to correlate with riverine freshwater influx during summer, both RI2 and RI1 cores show reduced Ba/Ca ratios in summer and enhanced Ba/Ca in winter (Fig. 4).

Continuous wavelet transform (CWT) indicates that similar to Sr/Ca and SST, Ba/Ca ratios in the long RI2 core shows a consistent annual cyclicity over the analysed period from 1976 to 2016 (Fig. 5 a,b,c). A cross wavelet transform (XWT) of Ba/Ca with SST and Sr/Ca indicates anti-phasing of Ba/Ca with SST and in-phasing with Sr/Ca with high common power in the 1 year band (Fig. 5 d, e). Significantly strong (at 95% confidence level) inverse covariance of Ba/Ca with SST and positive covariance with Sr/Ca in the 1year band was observed in wavelet coherence (WTC) analysis (Fig. 5 f, g). Thus, wavelet analysis strongly suggests consistent timing of the RI2 Ba/Ca oscillation.

4. Discussion

Biogeochemical cycling of Ba in marine environments is controlled by several factors, including (i) riverine input, especially for coastal waters (Coffey et al., 1997), (ii) wind/wave associated sediment resuspension (Esslemont et al., 2004), (iii) upwelling (Lea et al., 1989), (iv) direct (active) uptake by phytoplankton and/or adsorption on the phytoplankton cell surface (passive) (Fisher et al., 1991; Sternberg et al., 2005), and (v) barite formation associated with phytoplankton death (Dehairs et al., 1980; Stroobants et al., 1991; Stecher and Kogut, 1999; Pyle et al., 2017). Incorporation of Ba into coral aragonite also is influenced by temperature (Gaetani and Cohen, 2006).

A major external source of Ba in coastal water is riverine input and the fluvial flux of dissolved Ba is significantly enhanced in low salinity estuarine regions due to desorption of Ba from river-introduced suspended clays by exchange with major cations in seawater (Hanor and Chan, 1977; Coffey et al., 1997; Nozaki et al., 2001). Distinct seasonal patterns in dissolved Ba in coastal water is expected due to seasonal variations in the magnitude of river discharge (Thomas et al., 2011) and was observed in coral skeleton time series data in several different geographic locations (McCulloch et al., 2003; Fleitmann et al., 2007; Jupiter et al., 2008; Moyer et al., 2012; Walther et al., 2013; Saha et al., 2018). Enhanced sediment delivery associated with catchment clearance and drought-breaking floods resulted in significant enrichment of Ba/Ca in a *Porites* sp. coral at Great Keppel Island (Saha et al., 2018), which is located in more open, but still coastal waters ~ 75 km north-west of Rat Island where it is influenced directly by the northward flowing Fitzroy River plumes (Alibert et al., 2003; Sinclair and McCulloch, 2004). Whilst Ba/Ca in the Great Keppel coral fluctuated with annual Fitzroy River discharge and showed more synchronous behaviour with discharge on a decadal timescale, no apparent link between seasonal river discharge (or rainfall) and Ba/Ca was recorded in the present study. Rather, RI1 and RI2 Ba/Ca time series

shows consistent seasonal fluctuation with winter maximum and summer minimum throughout the years analysed (Fig. 4). The distinct hydro-geographic positions of these two coral locations may partly explain the different behaviour of the Ba/Ca proxy. Great Keppel is exposed to open seawater with high hydraulic flushing and coral records lower Ba/Ca concentration [ranging from 3.57–7.21 μmol/mol with an average of 4.34 ± 0.42 (1σ) μmol/mol] relative to Rat Island coral [Ba/Ca in RI2 varied from 4.26 to 13.93 μmol/mol with a mean value of 7.40 ± 2.05 (1σ) μmol/mol] and therefore, is likely to capture episodic Ba/Ca pulses related to higher discharge. In contrast, restricted water turnover in PC likely results in more persistently turbid water with a saturated and elevated background of Ba concentration in seawater through the year and thus, summer pulses are effectively masked and other seasonal environmental factors drive the summer and winter oscillation of Ba/Ca. Anomalous oscillation of Ba/Ca uncorrelated with local river discharge was also reported in other studies (Sinclair, 2005b; Carriquiry and Horta-Puga, 2010; Chen et al., 2011; Lewis et al., 2012), showing that terrestrial runoff does not solely govern the complex marine biogeochemistry of Ba.

Resuspension of buried sediment by wind associated turbulence may result in desorption of Ba from resuspended sediment particles and can enhance water column dissolved Ba content (Esslemont et al., 2004). In some cases, Esslemont et al. (2004) did not find expected Ba/Ca spikes despite the wind speed being favourable for resuspension. However, tropical cyclones with high wind speed, which would be expected to resuspended sediments usually affect the eastern coast of Queensland during summer periods (from January to March) as shown in Fig. 4. Hence, wind induced resuspension cannot explain the temporal Ba/Ca patterns recorded in this study, wherein higher Ba/Ca ratios occur in winter, when the ocean is relatively calm (Fig. 4).

Seasonal upwelling into the GBR, which is enhanced during summer months (Furnas, 2011), may act as a significant source of Ba/Ca pulses in corals (Lea et al., 1989; Shen et al., 1992; Ourbak et al., 2006). Upwelling dynamics in the GBR are primarily controlled by the relative depth of the thermocline at the edge of the continental shelf. Therefore, offshore reefs are potentially influenced by the ingress of cold, nutrient-rich water up the slope to the shelf-break (Andrews and Gentien, 1982; Walther et al., 2013). Hence, Ba/Ca seasonality in nearshore RI1 and RI2 (~ 200 km from the continental shelf edge) with a summer minima is unlikely to be driven by regional upwelling.

Anti-correlation between temperature and Ba/Ca was observed in both experimentally precipitated aragonite (Dietzel et al., 2004; Gaetani and Cohen, 2006) and stained *Diploria labyrinthiformis* coral skeleton growing at ~15 m depth on the south terrace of Bermuda platform (Gaetani and Cohen, 2006). Differential partitioning of Ba and Ca in aragonite and fluctuation of precipitation efficiency (higher in summer) based on seasonal temperature variation was suggested as a potential cause of temperature dependency of Ba/Ca. The reported temperature dependency for *Diploria* coral skeleton is -0.213 µmol/mol per °C, which would equate to ~2 µmol/mol Ba/Ca variation over our composite SST range of ~20–29 °C (from 1976 to 2016). The same is true for a short (Jun 2016 to Apr 2017) *in situ* SST (AIMS temperature logger) record at Rat Island wherein seasonal SST varied in the range between 19.84 to 28.81°C (i.e., annual amplitude is 8.97 °C) with an average of 24.65 °C. The range of unsmoothed Ba/Ca variability for RI2 core is ~ 10 µmol/mol (from 4.26 to 13.93 µmol/mol). Ba/Ca–temperature relationships in corals may be taxon specific and temperature could have more influence on Ba incorporation into *Cyphastrea* than into *Diploria*, but such a great difference appears unlikely. Even though the range of long-term seasonal SST fluctuation at Rat Island could be slightly higher than the short *in situ* (at Rat Island) record of ~9 °C, the required abrupt fluctuation in temperature (~ 47 °C based on the

relationship of -0.213 µmol/mol Ba/Ca per °C) to compensate the recorded ~10 µmol/mol Ba/Ca variability is highly unrealistic. As long-term local seawater temperature data are not available, the commonly used SST proxy, i.e., Sr/Ca signatures in relatively slow growing Cyphastrea's skeleton can possibly be used to reconstruct SST. However, reconstruction of SST on a longer temporal scale (1976 to 2016) using linear regression between monthly Sr/Ca and monthly composite SST over the period of 1976 to 2016 [regression equation: Sr/Ca (mmol/mol) = 9.828 (± 0.473) − 0.02861 (± 0.019) × SST (ºC); r = - 0.671; $p < 0.01$, root mean square of residuals (RRMS) = 2.63 ºC] (Fig. S2) provides an unrealistic peak-to-peak SST amplitude of ~20 °C [from 14.81 to 35.32 ºC with an average of 24.66 ± 3.55 (1σ)] at Rat Island that occurs in tidal pass. This indicates that skeletal Sr/Ca signals also were modulated partially by other drivers. Sr/Ca signals in *Cyphastrea* could be influenced by the coastal proximity wherein local runoff may have affected the Sr/Ca in the turbid water of Rat Island (Shen et al., 1996; Marshall and McCulloch, 2002; Fallon et al., 2003). Other biological factors (so called "vital effects") are also thought to modulate the skeletal Sr/Ca signatures in corals (De Villiers et al., 1994; De Villiers et al., 1995; Allison and Finch, 2004; Sinclair, 2005a; Sinclair et al., 2006; Saenger et al., 2008; Cohen and Gaetani, 2010; Grove et al., 2013; Deng et al., 2014), and slower growing corals, like *Cyphastrea*, are more susceptible to such vital effects (Deng et al., 2014). Here, annual mean Sr/Ca in RI2 was positively influenced by the annual extension rate (Fig. S3). Similar positive extension rate effects on coral Sr/Ca records have been reported in other corals (Grove et al., 2013; Deng et al., 2014). A systematic increase in Sr/Ca with increasing abiogenic aragonite crystal growth and a decrease of this elemental ratio with decreasing crystal growth also was reported by Cohen and Gaetani (2010). Thus, although the annual cyclicity of Sr/Ca derived from *Cyphastrea* satisfies the major goal of chronology development for this study, utilization of this proxy for SST reconstruction requires further investigation. Regardless, temperature

could be responsible for some of the seasonal Ba/Ca fluctuation in *Cyphastrea*, but temperature alone is unlikely to account for the high amplitude of the Ba/Ca signals.

Excess nutrients are problematic for reef ecosystems (Hallock and Schlager, 1986; Koop et al., 2001; Fabricius, 2005; D'Angelo and Wiedenmann, 2014; Vega Thurber et al., 2014; Humanes et al., 2016) and their dominant source in coastal waters is the terrestrial supply, which is enhanced anthropogenically by fertilizers in runoff from agriculture and accelerated soil erosion caused by land use change (Furnas and Mitchell, 2000; Wooldridge et al., 2006; Brodie et al., 2012). On a seasonal scale, delivery of nutrients (both dissolved and particulate) in coastal water is highly variable and generally increases with higher discharge during wet summer intervals (Brodie et al., 2007; Devlin et al., 2012; Lønborg et al., 2017). Summer enrichment of nutrients triggers the abundant production of phytoplankton communities in Port Curtis (Currie and Small, 2005) similar to other coastal regions along the GBR (Furnas et al., 1990; Furnas et al., 2005; Schaffelke et al., 2012). An outstanding feature of Ba/Ca time series in RI1 and RI2 is its seasonal regularity throughout the years analysed, indicating a dominant influence of seasonal environmental drivers (Fig. 4 and 5). Ba/Ca data are anti-phased with seawater chlorophyll concentration, which reflects phytoplankton biomass, suggesting a possible influence of ocean biology on the Ba/Ca cycle (Fig. 6). During spring, SST begins to rise, solar exposure has been increasing for several months, magnitude of rainfall, discharge, and nutrient supply (indicated as dissolved phosphate) to the sheltered water of Port Curtis starts a gradual rise, and there is an extended calm period with low wind and tidal flushing (Fig. 7). All of these conditions (Revelante and Gilmartin, 1982; Revelante et al., 1982; Furnas et al., 1990; Bell et al., 1999; Sinclair, 2005b) are favourable for phytoplankton blooms (indicated as chlorophyll in Fig. 7) in the semi-enclosed coastal embayment of Port Curtis.

Dynamics of marine Ba may be related to active or passive biological drawdown of dissolved Ba during blooming seasons and indirect biologically mediated precipitation of Ba as the mineral barite ($BaSO_4$) in super saturated micro-environments associated with decaying phytoplankton during post-bloom periods. Active uptake of Ba by live phytoplankton (Fisher et al., 1991) and/or adsorption (i.e., passive) on phytoplankton cell surfaces (Sternberg et al., 2005) may lead to a depletion of dissolved Ba. Laboratory experiments show that diatom cells take up Ba in direct proportion to the ambient seawater concentration and localization of most of the absorbed Ba is associated with the frustules (Fisher et al., 1991). Linkage between elevated particulate Ba (not present as barite) and higher biomass in the southern ocean (Cardinal et al., 2005) and culture experiments with the diatom (Sternberg et al., 2005) suggested absorption of Ba onto biogenic matter. A steady decline in Ba/Ca in both RI1 and RI2 cores is coupled with an increase in chlorophyll concentration from early-spring, which may be attributed to progressive increase in sorptive (adsorption and absorption) removal of Ba with increased plankton abundance during the spring bloom (Fig. 7). Semi-confined water of this shallow embayment may trap significant amounts of phytoplankton due to hydrodynamic restriction. Similar Ba/Ca behaviour with winter maxima and summer minima was observed in a short time series record in a *Porites lutea* colony from a shallow sheltered embayment of Cow and Calf Island (Whitsunday region, central GBR) and was attributed to planktic influence (Fig. S4) (Sinclair, 2005b).

Formation of marine barite is not associated with live phytoplankton (Bishop, 1988; Stroobants et al., 1991) but with dead phytoplankton, because most sea water is under-saturated with respect to barite ($BaSO_4$) (Church and Wolgemuth, 1972; Monnin et al., 1999; Rushdi et al., 2000) and decaying phytoplankton and fecal material provide a sulfate-rich micro-environment favourable for barite micro-crystal precipitation (Dehairs et al., 1980; Bishop, 1988; Stroobants et al., 1991; Jeandel et al., 2000; Ganeshram et al., 2003; Pyle et al.,

2017). After barite is precipitated in the biogenic detritus, coral may ingest the Ba-rich particles as food sources, or Ba may remineralize while barite particles descend though the water column, or barite particles may be buried in the sediment (Chan et al., 1977; Dehairs et al., 1980; Bruland, 1983; Stroobants et al., 1991; Jacquet et al., 2007). Planktic blooms during spring and summer should have increased Ba/Ca ratios if *Cyphastrea* either ingested Ba-enriched particles or barite was remineralized during sinking. However, Ba/Ca peaks of RI1 and RI2 occur in winter following a decrease from the beginning of spring and they reaches their lowest values in summer (Fig. 7). Significant removal of dissolved Ba through the conversion to particulate barite at the end of diatom-dominated spring bloom has been observed in both oceanic (Bishop, 1988; Stroobants et al., 1991) and estuarine (Stecher and Kogut, 1999; Pyle et al., 2017) environments. Higher availability of micro-environments in abundant depth assemblages during post-bloom stages may accelerate the formation of barite and outflux of dissolved Ba from the water column around Rat Island as is observed in Cyphastrea's Ba/Ca seasonal records (Fig. 7). The amplitude of Ba/Ca in RI1 is relatively lower than RI2 (Fig. 7) because RI2 Ba/Ca is the long-term (over the period of 1976 to 2016) seasonal average of monthly values, whereas RI1 Ba/Ca represent only a short-term (2002 to 2006) average of monthly values, when Ba/Ca was supressed in both cores (Fig. 4).

Overall, a cumulative effect of bioconcentration of Ba during the phytoplankton blooming period and removal of barite particles during post-bloom phytoplankton decaying stage may explain the seasonality of coralline Ba/Ca with its remarkable decrease from early spring to late summer (Fig. 7). Importantly, the greatest flux of new terrestrial Ba would be expected in the summer high discharge intervals, but dissolved Ba is low at that time based on the coral record.

5. Conclusions

Changing water quality due to increased anthropogenic pressures is a major driver for declining inshore coral communities along the GBR. Proxy-based reconstructions are unequivocally important for extending our knowledge of changes in water quality beyond the instrumental record so as to better predict the future of coral communities, not only in the GBR, but in other locations in the world. The limited spatial distribution of commonly used *Porites* species indicates the need for alternative species for investigating palaeoenvironment, especially in the inshore sub-tropical high latitude. The simple skeletal architecture and skeletal microstructure of *Cyphastrea* similar to those of *Porites*. That combined with wide geographic distribution (both tropical and sub-tropical region of the GBR) (Veron, 2000), extended growth record, clear annual density banding, and seasonally resolved Sr/Ca signals suggest the high potential for *Cyphastrea* to be used as a novel palaeoenvironmental archive. However, the commonly used coralline Ba/Ca proxy is influenced by multiple environmental and climatic drivers, and thus, complicates the interpretation of targeted water quality drivers (e.g., terrestrial sediment runoff). The long-term Ba/Ca record in *Cyphastrea* from Rat Island, GBR shows for the first time that consistent seasonal cyclicity in an inshore coral is controlled not by terrestrial input associated with runoff, but by associated marine biochemical cycles. Although the RI1 and RI2 coral cores are located in close proximity to the Calliope and Boyne river mouths, oscillation of Ba/Ca signals was not directly linked to the expected environmental drivers: terrestrial discharge and/or rainfall. Rather, we found an indirect link to discharge through a control of nutrient supply and associated phytoplankton productivity. Geochemical cycling of Ba in the semi-enclosed embayment of Port Curtis is likely to be controlled by seasonal phytoplankton dynamics that are themselves controlled in part by terrestrial nutrient supply. A remarkable decrease in skeletal Ba/Ca from early spring to late summer may be a cumulative effect of drawdown of Ba through direct uptake by live

phytoplankton and/or adsorption on the cell surface during the spring bloom period and sinking of barite minerals formed in special micro-environments of decaying phytoplankton during post-bloom stages. Importantly, this drawdown occurs during the expected peak delivery of Ba from runoff. Gradual reduction in abundance of planktic biomass from autumn through winter results in increased Ba/Ca with peaks in late winter. Hydrographic conditions of Port Curtis with restricted hydraulic flushing may act as a natural trap for phytoplankton, which exerts an eventual dominant control on dissolved Ba content. Thus, whereas Ba/Ca may serve as a direct proxy for runoff in some more open geographic settings, it may be modulated into an antiphase relationship by phytoplankton in other settings, such as Port Curtis. We recommend that physicochemical oceanographic conditions of the coral sampling site should be taken into account for utilizing coralline Ba/Ca proxy to understand long-term water quality linked to terrestrial runoff. To better understand the dynamics of Ba in semi-enclosed estuarine systems like Port Curtis, future research should investigate the seasonal variability of dissolved Ba, nutrient and chlorophyll concentrations, and their connectivity in semiconfined coastal water. Further study on the Ba/Ca–temperature calibration is also recommended for *Cyphastrea* to isolate the influence of temperature on the variability of Ba/Ca.

Acknowledgements

This work was partially funded by Tropical Ecosystem Project 1.3 led by Zhao and others, ARC Discovery grant DP120101793 led by Webb and others, Stanley Gray Fellowship from Institute of Marine, Engineering, Science and Technology (IMarEST), and an Australian Government Research Training Program Scholarship. We thank James Sadler, Tara R. Clark and Peran Bray for their help in organizing and assisting during field trip. We are grateful to the anonymous reviewers for their useful comments and suggestions in improving this manuscript. Sr/Ca and Ba/Ca data for RI2 and RI1 cores are presented as Data Table 1 and 2 at the end of supporting file.

References

Alibert, C., Kinsley, L., Fallon, S.J., McCulloch, M.T., Berkelmans, R., McAllister, F., 2003. Source of trace element variability in Great Barrier Reef corals affected by the Burdekin flood plumes. Geochim. Cosmochim. Acta 67, 231-246.

Allison, N., Finch, A.A., 2004. High- resolution Sr/Ca records in modern Porites lobata corals: Effects of skeletal extension rate and architecture. Geochem. Geophys. Geosyst. 5.

Andrews, J.C., Gentien, P., 1982. Upwelling as a source of nutrients for the Great Barrier Reef ecosystems: a solution to Darwin's question? Mar. Ecol. Prog. Ser. 8, 257-269.

Ayling, A., Ayling, A., Ceccarelli, D., 2012. The impacts of dredge spoil dumping on fringing coral reefs around Facing Island. Report prepared for Gladstone Ports Corporation Limited, Sea Research, BN 2400509; ABN 51 594 242 720.

Beck, J.W., Edwards, R.L., Ito, E., Taylor, F.W., Recy, J., Rougerie, F., Joannot, P., Henin, C., 1992. Sea-surface temperature from coral skeletal strontium/calcium ratios. Science 257, 644-647.

Bell, P., Elmetri, I., Uwins, P., 1999. Nitrogen fixation by Trichodesmium spp. in the Central and Northern Great Barrier Reef Lagoon: relative importance of the fixed-nitrogen load. Mar. Ecol. Prog. Ser. 186, 119-126.

Bishop, J.K.B., 1988. The barite-opal-organic carbon association in oceanic particulate matter. Nature 332, 341-343.

Bolton, A., Goodkin, N., Hughen, K., Ostermann, D., Vo, S., Phan, H., 2014. Paired *Porites* coral Sr/Ca and $\delta^{18}O$ from the western South China Sea: Proxy calibration of sea surface temperature and precipitation. Palaeogeogr. Palaeoclimatol. Palaeoecol. 410, 233-243.

Brodie, J., De'Ath, G., Devlin, M., Furnas, M., Wright, M., 2007. Spatial and temporal patterns of near-surface chlorophyll a in the Great Barrier Reef lagoon. Mar. Freshwater Res. 58, 342-353.

Brodie, J., Kroon, F., Schaffelke, B., Wolanski, E., Lewis, S., Devlin, M., Bohnet, I., Bainbridge, Z., Waterhouse, J., Davis, A., 2012. Terrestrial pollutant runoff to the Great Barrier Reef: an update of issues, priorities and management responses. Mar. Pollut. Bull. 65, 81-100.

Brodie, J.E., Devlin, M., Haynes, D., Waterhouse, J., 2011. Assessment of the eutrophication status of the Great Barrier Reef lagoon (Australia). Biogeochemistry 106, 281-302.

Bruland, K.W., 1983. Trace elements in sea-water. In: Riley, P.J., Chester, R. (Eds.), Chemical oceanography, pp. 157-220.

Cardinal, D., Savoye, N., Trull, T.W., André, L., Kopczynska, E.E., Dehairs, F., 2005. Variations of carbon remineralisation in the Southern Ocean illustrated by the Ba xs proxy. Deep Sep Res. PT I 52, 355-370.

Carilli, J.E., Norris, R.D., Black, B.A., Walsh, S.M., McField, M., 2009. Local stressors reduce coral resilience to bleaching. PLoS one 4, e6324.

Carriquiry, J.D., Horta-Puga, G., 2010. The Ba/Ca record of corals from the Southern Gulf of Mexico: Contributions from land-use changes, fluvial discharge and oil-drilling muds. Mar. Pollut. Bull. 60, 1625-1630.

Carroll, J., Falkner, k.K., Brown, E.T., Moore, W.S., 1993. The role of the Ganges-Brahmaputra mixing zone in supplying barium and ^{226}Ra to the Bay of Bengal. Geochim. Cosmochim. Acta 57, 2981-2990.

Chan, L., Drummond, D., Edmond, J., Grant, B., 1977. On the barium data from the Atlantic GEOSECS expedition. Deep Sea Res. 24, 613-649.

Chan, L.H., Edmond, J.M., Stallard, R.F., Broecker, W.S., Chung, Y.C., Weiss, R.F., Ku, T.L., 1976. Radium and barium at GEOSECS stations in the Atlantic and Pacific. Earth. Planet. Sci. Lett. 32, 258-267.

Chen, T., Yu, K., Li, S., Chen, T., Shi, Q., 2011. Anomalous Ba/Ca signals associated with low temperature stresses in *Porites* corals from Daya Bay, northern South China Sea. J. Environ. Sci. 23, 1452-1459.

Church, T.M., Wolgemuth, K., 1972. Marine barite saturation. Earth. Planet. Sci. Lett. 15, 35-44.

Clark, T.R., Roff, G., Zhao, J.-x., Feng, Y.-x., Done, T.J., McCook, L.J., Pandolfi, J.M., 2017. U-Th dating reveals regional-scale decline of branching *Acropora* corals on the Great Barrier Reef over the past century. Proc. Natl. Acad. Sci. 114, 10350-10355.

Coffey, M., Dehairs, F., Collette, O., Luther, G., Church, T., Jickells, T., 1997. The behaviour of dissolved barium in estuaries. Estuar. Coast Shelf Sci. 45, 113-121.

Cohen, A., Gaetani, G.A., 2010. Ion partitioning and the geochemistry of coral skeletons: solving the mystery of the vital effect. EMU Notes in Mineralogy 11, 377-397.

Conaghan, P.J., 1966. Sediments and sedimentary processes in Gladstone Harbour, Queensland. University of Queensland Press, St Lucia 6, 1-52.

Cunning, R., Baker, A.C., 2013. Excess algal symbionts increase the susceptibility of reef corals to bleaching. Nature Clim. Change 3, 259-262.

Currie, D.R., Small, K.J., 2005. Macrobenthic community responses to long-term environmental change in an east Australian sub-tropical estuary. Estuar. Coast Shelf Sci. 63, 315-331.

D'Angelo, C., Wiedenmann, J., 2014. Impacts of nutrient enrichment on coral reefs: new perspectives and implications for coastal management and reef survival. Curr. Opin. Environ. Sust. 7, 82-93.

De'ath, G., Fabricius, K., 2010. Water quality as a regional driver of coral biodiversity and macroalgae on the Great Barrier Reef. Ecol. Appl. 20, 840-850.

De Villiers, S., Nelson, B.K., Chivas, A.R., 1995. Biological controls on coral Sr/Ca and $\delta^{18}O$ reconstructions of sea surface temperatures. Science 269, 1247-1249.

De Villiers, S., Shen, G.T., Nelson, B.K., 1994. The Sr/Ca-temperature relationship in coralline aragonite: Influence of variability in (Sr/Ca) seawater and skeletal growth parameters. Geochim. Cosmochim. Acta 58, 197-208.

De'ath, G., Fabricius, K.E., Sweatman, H., Puotinen, M., 2012. The 27–year decline of coral cover on the Great Barrier Reef and its causes. Proc. Natl. Acad. Sci. 109, 17995-17999.

Dehairs, F., Chesselet, R., Jedwab, J., 1980. Discrete suspended particles of barite and the barium cycle in the open ocean. Earth. Planet. Sci. Lett. 49, 528-550.

DeLong, K.L., Flannery, J.A., Maupin, C.R., Poore, R.Z., Quinn, T.M., 2011. A coral Sr/Ca calibration and replication study of two massive corals from the Gulf of Mexico. Palaeogeogr. Palaeoclimatol. Palaeoecol. 307, 117-128.

DeLong, K.L., Quinn, T.M., Taylor, F.W., Shen, C.-C., Lin, K., 2013. Improving coral-base paleoclimate reconstructions by replicating 350years of coral Sr/Ca variations. Palaeogeogr. Palaeoclimatol. Palaeoecol. 373, 6-24.

Deng, W., Wei, G., McCulloch, M., Xie, L., Liu, Y., Zeng, T., 2014. Evaluation of annual resolution coral geochemical records as climate proxies in the Great Barrier Reef of Australia. Coral Reefs 33, 965-977.

Devlin, M., McKinna, L., Alvarez-Romero, J., Petus, C., Abott, B., Harkness, P., Brodie, J., 2012. Mapping the pollutants in surface riverine flood plume waters in the Great Barrier Reef, Australia. Mar. Pollut. Bull. 65, 224-235.

Dietzel, M., Gussone, N., Eisenhauer, A., 2004. Co-precipitation of Sr^{2+} and Ba^{2+} with aragonite by membrane diffusion of CO_2 between 10 and 50 °C. Chem. Geol. 203, 139-151.

Dikou, A., van Woesik, R., 2006. Survival under chronic stress from sediment load: Spatial patterns of hard coral communities in the southern islands of Singapore. Mar. Pollut. Bull. 52, 7-21.

Erftemeijer, P.L., Riegl, B., Hoeksema, B.W., Todd, P.A., 2012. Environmental impacts of dredging and other sediment disturbances on corals: a review. Mar. Pollut. Bull. 64, 1737-1765.

Esslemont, G., Russell, R., Maher, W., 2004. Coral record of harbour dredging: Townsville, Australia. J. Mar. Sys. 52, 51-64.

Fabricius, K., Wolanski, E., 2000. Rapid smothering of coral reef organisms by muddy marine snow. Estuar. Coast Shelf Sci. 50, 115-120.

Fabricius, K.E., 2005. Effects of terrestrial runoff on the ecology of corals and coral reefs: review and synthesis. Mar. Pollut. Bull. 50, 125-146.

Fallon, S.J., McCulloch, M.T., Alibert, C., 2003. Examining water temperature proxies in *Porites* corals from the Great Barrier Reef: a cross-shelf comparison. Coral Reefs 22, 389-404.

Fisher, N.S., Guillard, R.R., Bankston, D.C., 1991. The accumulation of barium by marine phytoplankton grown in culture. J. Mar. Res. 49, 339-354.

Fleitmann, D., Dunbar, R.B., McCulloch, M., Mudelsee, M., Vuille, M., McClanahan, T.R., Cole, J.E., Eggins, S., 2007. East African soil erosion recorded in a 300 year old coral colony from Kenya. Geophy. Res. Lett. 34.

Flores, F., Hoogenboom, M.O., Smith, L.D., Cooper, T.F., Abrego, D., Negri, A.P., 2012. Chronic exposure of corals to fine sediments: lethal and sub-lethal impacts. PloS one 7, e37795.

Furnas, M., Mitchell, A., 2000. Runoff of terrestrial sediment and nutrients into the Great Barrier Reef World Heritage Area, Oceanographic Processes of Coral Reefs: Physical and Biological Links in the Great Barrier Reef, pp. 37-52.

Furnas, M., Mitchell, A., Skuza, M., Brodie, J., 2005. In the other 90%: phytoplankton responses to enhanced nutrient availability in the Great Barrier Reef Lagoon. Mar. Pollut. Bull. 51, 253-265.

Furnas, M.J., 2011. Upwelling and coral reefs. In: Hopley, D. (Ed.), Encyclopedia of Modern Coral Reefs. Springer, pp. 1125-1128.

Furnas, M.J., Mitchell, A.W., Gilmartin, M., Revelante, N., 1990. Phytoplankton biomass and primary production in semi-enclosed reef lagoons of the central Great Barrier Reef, Australia. Coral Reefs 9, 1-10.

Gaetani, G.A., Cohen, A.L., 2006. Element partitioning during precipitation of aragonite from seawater: a framework for understanding paleoproxies. Geochim. Cosmochim. Acta 70, 4617-4634.

Gagan, M.K., Ayliffe, L.K., Hopley, D., Cali, J.A., Mortimer, G.E., Chappell, J., McCulloch, M.T., Head, M.J., 1998. Temperature and surface-ocean water balance of the mid-Holocene tropical western Pacific. Science 279, 1014-1018.

Ganeshram, R.S., François, R., Commeau, J., Brown-Leger, S.L., 2003. An experimental investigation of barite formation in seawater. Geochim. Cosmochim. Acta 67, 2599-2605.

GPC, 2014. Long term monitoring and management plan for sea disposal of maintenance dredge material 2013-2018, Gladstone Port Corporation.

Grinsted, A., Moore, J.C., Jevrejeva, S., 2004. Application of the cross wavelet transform and wavelet coherence to geophysical time series. Nonlinear Proc. Geoph. 11, 561-566.

Grove, C.A., Kasper, S., Zinke, J., Pfeiffer, M., Garbe-Schönberg, D., Brummer, G.-J.A., 2013. Confounding effects of coral growth and high SST variability on skeletal Sr/Ca: Implications for coral paleothermometry. Geochem. Geophys. Geosyst. 14, 1277-1293.

Hallock, P., Schlager, W., 1986. Nutrient excess and the demise of coral reefs and carbonate platforms. Palaios, 389-398.

Hanor, J.S., Chan, L.-H., 1977. Non-conservative behavior of barium during mixing of Mississippi River and Gulf of Mexico waters. Earth. Planet. Sci. Lett. 37, 242-250.

Hoegh-Guldberg, O., Mumby, P., Hooten, A., Steneck, R., Greenfield, P., Gomez, E., Harvell, C., Sale, P., Edwards, A., Caldeira, K., 2007. Coral reefs under rapid climate change and ocean acidification. science 318, 1737-1742.

Hopley, D., Smithers, S.G., Parnell, K., 2007. The geomorphology of the Great Barrier Reef: development, diversity and change. Cambridge University Press, Cambridge.

Hoppema, M., Dehairs, F., Navez, J., Monnin, C., Jeandel, C., Fahrbach, E., de Baar, H.J.W., 2010. Distribution of barium in the Weddell Gyre: Impact of circulation and biogeochemical processes. Mar. Chem. 122, 118-129.

Humanes, A., Noonan, S.H., Willis, B.L., Fabricius, K.E., Negri, A.P., 2016. Cumulative effects of nutrient enrichment and elevated temperature compromise the early life history stages of the coral Acropora tenuis. PloS one 11, e0161616.

Hunter, H.M., Walton, R.S., 2008. Land-use effects on fluxes of suspended sediment, nitrogen and phosphorus from a river catchment of the Great Barrier Reef, Australia. J. Hydrol. 356, 131-146.

Jacquet, S.H.M., Dehairs, F., Elskens, M., Savoye, N., Cardinal, D., 2007. Barium cycling along WOCE SR3 line in the Southern Ocean. Mar. Chem. 106, 33-45.

Jeandel, C., Tachikawa, K., Bory, A., Dehairs, F., 2000. Biogenic barium in suspended and trapped material as a tracer of export production in the tropical NE Atlantic (EUMELI sites). Mar. Chem. 71, 125-142.

Jones, R., Bessell-Browne, P., Fisher, R., Klonowski, W., Slivkoff, M., 2016. Assessing the impacts of sediments from dredging on corals. Mar. Pollut. Bull. 102, 9-29.

Jupiter, S., Roff, G., Marion, G., Henderson, M., Schrameyer, V., McCulloch, M., Hoegh-Guldberg, O., 2008. Linkages between coral assemblages and coral proxies of terrestrial exposure along a cross-shelf gradient on the southern Great Barrier Reef. Coral Reefs 27, 887-903.

Kelly, A.E., Reuer, M.K., Goodkin, N.F., Boyle, E.A., 2009. Lead concentrations and isotopes in corals and water near Bermuda, 1780–2000. Earth. Planet. Sci. Lett. 283, 93-100.

Kiem, A.S., Franks, S.W., 2004. Multi- decadal variability of drought risk, eastern Australia. Hydrol. Process. 18, 2039-2050.

Kiem, A.S., Franks, S.W., Kuczera, G., 2003. Multi- decadal variability of flood risk. Geophy. Res. Lett. 30.

King, B., McAllister, F., Wolanski, E., Done, T., Spagnol, S., 2001. River plume dynamics in the central Great Barrier Reef, Oceanographic Processes of Coral Reefs: Physical and Biological Links in the Great Barrier Reef, pp. 145-159.

Koop, K., Booth, D., Broadbent, A., Brodie, J., Bucher, D., Capone, D., Coll, J., Dennison, W., Erdmann, M., Harrison, P., 2001. ENCORE: the effect of nutrient enrichment on coral reefs. Synthesis of results and conclusions. Mar. Pollut. Bull. 42, 91-120.

Kroon, F.J., Kuhnert, P.M., Henderson, B.L., Wilkinson, S.N., Kinsey-Henderson, A., Abbott, B., Brodie, J.E., Turner, R.D., 2012. River loads of suspended solids, nitrogen, phosphorus and herbicides delivered to the Great Barrier Reef lagoon. Mar. Pollut. Bull. 65, 167-181.

LaVigne, M., Grottoli, A.G., Palardy, J.E., Sherrell, R.M., 2016. Multi-colony calibrations of coral Ba/Ca with a contemporaneous in situ seawater barium record. Geochim. Cosmochim. Acta 179, 203-216.

Lea, D.W., Shen, G.T., Boyle, E.A., 1989. Coralline barium records temporal variability in equatorial Pacific upwelling. Nature 340, 373-376.

Lewis, S., Brodie, J., McCulloch, M., Mallela, J., Jupiter, S., Stuart Williams, H., Lough, J., Matson, E., 2012. An assessment of an environmental gradient using coral geochemical records, Whitsunday Islands, Great Barrier Reef, Australia. Mar. Pollut. Bull. 65, 306-319.

Lewis, S.E., Shields, G.A., Kamber, B.S., Lough, J.M., 2007. A multi-trace element coral record of land-use changes in the Burdekin River catchment, NE Australia. Palaeogeogr. Palaeoclimatol. Palaeoecol. 246, 471-487.

Li, Y.-H., Chan, L.-H., 1979. Desorption of Ba and ^{226}Ra from river-borne sediments in the Hudson estuary. Earth. Planet. Sci. Lett. 43, 343-350.

Lønborg, C., Doyle, J., Furnas, M., Menendez, P., Benthuysen, J.A., Carreira, C., 2017. Seasonal organic matter dynamics in the Great Barrier Reef lagoon: Contribution of carbohydrates and proteins. Cont. Shelf Res. 138, 95-105.

Lough, J., Lewis, S., Cantin, N., 2015. Freshwater impacts in the central Great Barrier Reef: 1648–2011. Coral Reefs 34, 739-751.

Marshall, J.F., McCulloch, M.T., 2002. An assessment of the Sr/Ca ratio in shallow water hermatypic corals as a proxy for sea surface temperature. Geochim. Cosmochim. Acta 66, 3263-3280.

McCulloch, M., Fallon, S., Wyndham, T., Hendy, E., Lough, J., Barnes, D., 2003. Coral record of increased sediment flux to the inner Great Barrier Reef since European settlement. Nature 421, 727-730.

Monnin, C., Jeandel, C., Cattaldo, T., Dehairs, F., 1999. The marine barite saturation state of the world's oceans. Mar. Chem. 65, 253-261.

Montaggioni, L.F., Le Cornec, F., Corrège, T., Cabioch, G., 2006. Coral barium/calcium record of mid-Holocene upwelling activity in New Caledonia, South-West Pacific. Palaeogeogr. Palaeoclimatol. Palaeoecol. 237, 436-455.

Moyer, R., Grottoli, A., Olesik, J., 2012. A multi-proxy record of terrestrial inputs to the coastal ocean using minor and trace elements (Ba/Ca, Mn/Ca, Y/Ca) and carbon isotopes ($\delta^{13}C$, $\Delta^{14}C$) in a nearshore coral from Puerto Rico. Paleoceanography 27, PA3205.

Nothdurft, L.D., Webb, G.E., 2007. Microstructure of common reef-building coral genera *Acropora*, *Pocillopora*, *Goniastrea* and *Porites*: constraints on spatial resolution in geochemical sampling. Facies 53, 1-26.

Nozaki, Y., Yamamoto, Y., Manaka, T., Amakawa, H., Snidvongs, A., 2001. Dissolved barium and radium isotopes in the Chao Phraya River estuarine mixing zone in Thailand. Cont. Shelf Res. 21, 1435-1448.

Ourbak, T., Corrège, T., Malaizé, B., Le Cornec, F., Charlier, K., Peypouquet, J.P., 2006. A high- resolution investigation of temperature, salinity, and upwelling activity proxies in corals. Geochem. Geophys. Geosyst. 7.

Packett, R., Dougall, C., Rohde, K., Noble, R., 2009. Agricultural lands are hot-spots for annual runoff polluting the southern Great Barrier Reef lagoon. Mar. Pollut. Bull. 58, 976-986.

Paillard, D., Labeyrie, L., Yiou, P., 1996. Macintosh program performs time- series analysis. Eos, Transactions American Geophysical Union 77, 379-379.

Pastorok, R.A., Bilyard, G.R., 1985. Effects of sewage pollution on coral-reef communities. Mar. Ecol. Prog. Ser. 21, 175-189.

Petus, C., Devlin, M., 2012. Using satellite maps to document the extent of sediment plumes associated with the dredging activity in Gladstone Port's western basin, QLD. Queensland Rep, 1-46.

Potts, D., Done, T., Isdale, P., Fisk, D., 1985. Dominance of a coral community by the genus Porites (Scleractinia). Mar. Ecol. Prog. Ser., 79-84.

Pyle, K.M., Hendry, K.R., Sherrell, R.M., Meredith, M.P., Venables, H., Lagerström, M., Morte-Ródenas, A., 2017. Coastal barium cycling at the West Antarctic Peninsula. Deep Sea Research Part II: Topical Studies in Oceanography 139, 120-131.

Reuer, M.K., Boyle, E.A., Cole, J.E., 2003. A mid-twentieth century reduction in tropical upwelling inferred from coralline trace element proxies. Earth. Planet. Sci. Lett. 210, 437-452.

Revelante, N., Gilmartin, M., 1982. Dynamics of phytoplankton in the Great Barrier Reef Lagoon. J. Plankton Res. 4, 47-76.

Revelante, N., Williams, W.T., Bunt, J.S., 1982. Temporal and spatial distribution of diatoms, dinoflagellates and trichodesmium in waters of the Great Barrier Reef. J. Exp. Mar. Biol. Ecol. 63, 27-45.

Rodriguez-Ramirez, A., Grove, C.A., Zinke, J., Pandolfi, J.M., Zhao, J.-x., 2014. Coral luminescence identifies the Pacific Decadal Oscillation as a primary driver of river runoff variability impacting the southern Great Barrier Reef. PloS one 9, e84305.

Rogers, C.S., 1990. Responses of coral reefs and reef organisms to sedimentation. Mar. Ecol. Prog. Ser. 62, 185-202.

Rushdi, A.I., McManus, J., Collier, R.W., 2000. Marine barite and celestite saturation in seawater. Mar. Chem. 69, 19-31.

Sadler, J., Webb, G.E., Leonard, N.D., Nothdurft, L.D., Clark, T.R., 2016. Reef core insights into mid- Holocene water temperatures of the southern Great Barrier Reef. Paleoceanography 31, 1395-1408.

Saenger, C., Cohen, A.L., Oppo, D.W., Hubbard, D., 2008. Interpreting sea surface temperature from strontium/calcium ratios in Montastrea corals: Link with growth rate and implications for proxy reconstructions. Paleoceanography 23, PA3102.

Saha, N., Rodriguez-Ramirez, A., Nguyen, A.D., Clark, T.R., Zhao, J.X., Webb, G.E., 2018. Seasonal to decadal scale influence of environmental drivers on Ba/Ca and Y/Ca in coral aragonite from the southern Great Barrier Reef. Sci. Total Environ. 639, 1099-1109.

Saha, N., Webb, G.E., Zhao, J.-X., 2016. Coral skeletal geochemistry as a monitor of inshore water quality. Sci. Total Environ. 566–567, 652-684.

Schaffelke, B., Carleton, J., Skuza, M., Zagorskis, I., Furnas, M.J., 2012. Water quality in the inshore Great Barrier Reef lagoon: Implications for long-term monitoring and management. Mar. Pollut. Bull. 65, 249-260.

Seabrook, L., McAlpine, C., Fensham, R., 2006. Cattle, crops and clearing: regional drivers of landscape change in the Brigalow Belt, Queensland, Australia, 1840–2004. Landscape Urban Plan. 78, 373-385.

Seabrook, L., McAlpine, C., Fensham, R., 2007. Spatial and temporal analysis of vegetation change in agricultural landscapes: A case study of two brigalow (*Acacia harpophylla*) landscapes in Queensland, Australia. Agr. Ecosyst. Environ. 120, 211-228.

Shannon, R.t., 1976. Revised effective ionic radii and systematic studies of interatomic distances in halides and chalcogenides. Acta Crystallogr. Sec. A 32, 751-767.

Shen, C.-C., Lee, T., Chen, C.-Y., Wang, C.-H., Dai, C.-F., Li, L.-A., 1996. The calibration of D [Sr/Ca] versus sea surface temperature relationship for *Porites* corals. Geochim. Cosmochim. Acta 60, 3849-3858.

Shen, G.T., Cole, J.E., Lea, D.W., Linn, L.J., McConnaughey, T.A., Fairbanks, R.G., 1992. Surface ocean variability at Galapagos from 1936–1982: calibration of geochemical tracers in corals. Paleoceanography 7, 563-588.

Sinclair, D., Williams, B., Risk, M., 2006. A biological origin for climate signals in corals—Trace element "vital effects" are ubiquitous in Scleractinian coral skeletons. Geophy. Res. Lett. 33, L17707.

Sinclair, D.J., 2005a. Correlated trace element "vital effects" in tropical corals: a new geochemical tool for probing biomineralization. Geochim. Cosmochim. Acta 69, 3265-3284.

Sinclair, D.J., 2005b. Non-river flood barium signals in the skeletons of corals from coastal Queensland, Australia. Earth. Planet. Sci. Lett. 237, 354-369.

Sinclair, D.J., McCulloch, M.T., 2004. Corals record low mobile barium concentrations in the Burdekin River during the 1974 flood: evidence for limited Ba supply to rivers? Palaeogeogr. Palaeoclimatol. Palaeoecol. 214, 155-174.

Stecher, H.A., Kogut, M.B., 1999. Rapid barium removal in the Delaware estuary. Geochim. Cosmochim. Acta 63, 1003-1012.

Sternberg, E., Tang, D., Ho, T.-Y., Jeandel, C., Morel, F.M.M., 2005. Barium uptake and adsorption in diatoms. Geochim. Cosmochim. Acta 69, 2745-2752.

Stroobants, N., Dehairs, F., Goeyens, L., Vanderheijden, N., Van Grieken, R., 1991. Barite formation in the Southern Ocean water column. Mar. Chem. 35, 411-421.

Thomas, H., Shadwick, E., Dehairs, F., Lansard, B., Mucci, A., Navez, J., Gratton, Y., Prowe, F., Chierici, M., Fransson, A., 2011. Barium and carbon fluxes in the Canadian Arctic Archipelago. J. Geophys. Res: Oceans 116, C00G08.

Thorburn, P.J., Wilkinson, S.N., Silburn, D.M., 2013. Water quality in agricultural lands draining to the Great Barrier Reef: A review of causes, management and priorities. Agr. Ecosyst. Environ. 180, 4-20.

Torrence, C., Compo, G.P., 1998. A practical guide to wavelet analysis. B. Am. Meteorol. Soc. 79, 61-78.

Vega Thurber, R.L., Burkepile, D.E., Fuchs, C., Shantz, A.A., McMinds, R., Zaneveld, J.R., 2014. Chronic nutrient enrichment increases prevalence and severity of coral disease and bleaching. Glob. Change. Biol. 20, 544-554.

Verdon, D.C., Wyatt, A.M., Kiem, A.S., Franks, S.W., 2004. Multidecadal variability of rainfall and streamflow: Eastern Australia. Water Resour. Res. 40.

Veron, J., 2000. Corals of the World, vol. 3. Australian Institute of Marine Science, Townsville, Queensland, Australia.

Wagner, D.E., Kramer, P., Van Woesik, R., 2010. Species composition, habitat, and water quality influence coral bleaching in southern Florida. Mar. Ecol. Prog. Ser. 408, 65-78.

Wallace, C.C., Fellegara, I., Muir, P.R., Harrison, P.L., 2009. The scleractinian corals of Moreton Bay, eastern Australia: high latitude, marginal assemblages with increasing species richness. Memoirs of the Queensland Museum 54, 1-118.

Walther, B.D., Kingsford, M.J., McCulloch, M.T., 2013. Environmental records from Great Barrier Reef corals: inshore versus offshore drivers. PloS one 8, e77091.

Weber, M., de Beer, D., Lott, C., Polerecky, L., Kohls, K., Abed, R.M., Ferdelman, T.G., Fabricius, K.E., 2012. Mechanisms of damage to corals exposed to sedimentation. Proc. Natl. Acad. Sci. 109, E1558-E1567.

Witt, C., Teakle, I., Jorissen, J., 2009. Gladstone Western Basin EIS - Numerical Modelling Studies Gladstone Ports Corporation Australia

Wolgemuth, K., Broecker, W.S., 1970. Barium in sea water. Earth. Planet. Sci. Lett. 8, 372-378.

Wooldridge, S., Brodie, J., Furnas, M., 2006. Exposure of inner-shelf reefs to nutrient enriched runoff entering the Great Barrier Reef Lagoon: Post-European changes and the design of water quality targets. Mar. Pollut. Bull. 52, 1467-1479.

Wyndham, T., McCulloch, M., Fallon, S., Alibert, C., 2004. High-resolution coral records of rare earth elements in coastal seawater: biogeochemical cycling and a new environmental proxy. Geochim. Cosmochim. Acta 68, 2067-2080.

Figure captions

Fig. 1. (a) Map showing location of Rat Island in the Great Barrier Reef, Australia (inset). Geographical Information System (GIS) shapefiles were provided by the Great Barrier Reef Marine Park Authority (b) Coral sampling spot (red star) from southern side of the Rat Island. Google Earth image was used with permission from Google.

Fig. 2. (a, b) X-radiographs of Cyphastrea sp. coral slabs (RI1 and RI2) showing annual growth bands and sampling tracks (white lines). (c, d) Comparison of interpolated monthly Sr/Ca ratios of RI1 and RI2 with monthly resolution composite SST (HadISST—Jan 1976 to Oct 1981 and IGOSS SST—Nov 1981 to Jun 2016; see the text for SST data sources) over the period of Aug 2002 to Jul 2006 and Jan 1976 to Jun 2016, respectively. Maximum Sr/Ca corresponds to minimum SST and vice versa.

Fig. 3. SEM images of skeletal architecture and microstructures of Cyphastrea sp. coral skeleton, mounted in epoxy, polished and etched. (a) Transverse view (perpendicular to the growth direction) of vertically oriented corallites in Cyphastrea's skeleton showing the fundamental skeletal units - theca, radiating septa from wall and dissepiment. (b) Transverse section of a septa (outlined in a) showing multiple centers of rapid accretion (CRA) defining individual trabeculae. (c, d) Enlarged view of longitudinal section of a septa with CRA and surrounding thickening deposits (TD) projected from CRA. Note that entire skeleton is composed of fibrous aragonite.

Fig. 4. Ba/Ca signals recorded in RI1 and RI2 are compared with published Ba/Ca data showed linkage with terrestrial runoff (Top panel). Locations of Ba/Ca record along the GBR are shown in inset (a) in top panel. Box Whisker diagrams (inset b in top panel) show statistics of Ba/Ca from different locations of the GBR. The record of discharge (black line) for Calliope River, which directly influence the Rat Island is shown in bottom panel. The record of rainfall (grey line) from southern Curtis Island (station number 039241) over the period of 1976 to 2016 is also shown (bottom panel). See the text for discharge and rainfall data sources. Blue dashed lines indicate the timing of high discharge. [1]Jupiter et al., (2008), [2]McCulloch et al., (2003), [3]Walther et al., (2013), [4]Saha et al., (2018), [5,6]this study.

Fig. 5. (a–c) Continuous wavelet transform (CWT) of monthly SST, Sr/Ca (RI2) and Ba/Ca (RI2); (d and e) Cross wavelet transform (XWT) between monthly SST and Ba/Ca, and between monthly Sr/Ca and Ba/Ca; (f and g) Wavelet coherence (WTC) between monthly SST and Ba/Ca, and between monthly Sr/Ca and Ba/Ca. Period indicates year and black contours represent the significance at 95% confidence level. Right and left arrows indicate in-phase and anti-phase between two variables, respectively. Shaded region indicates the values outside of cone of influence (COI).

Fig. 6. Comparison of Ba/Ca time series (black dotted and solid lines indicate core RI1 and RI2, respectively) with in situ and satellite derived chlorophyll concentration data from different sources. Satellite derived (SeaWiFS sensor via GIOVANNI) chlorophyll-a concentration spanned from Sept 1997 to Oct 2010. In situ chlorophyll-a at Calliope River mouth and total chlorophyll at Pelican Island ranged from 1995 to 2001 and from 2007 to 2015, respectively. Data sources are mentioned in the text.

Fig. 7. Long-term seasonal averages of geochemical proxies [Ba/Ca (red solid line for core RI2 and red dotted line for core RI1) and Sr/Ca] and various environmental and climate parameters. Discharge, rainfall, composite SST, Ba/Ca and Sr/Ca data represent the average of monthly values of each parameter over the period of Jan 1976 to Jun 2016 (except for Ba/Ca in RI1, which spanned from Aug 2002 to Jul 2006). See the text for discharge, rainfall and SST data sources. Average of solar exposure and wind speed data spanned from 1990 to 2015 and 1976 to 2015, respectively. Solar exposure and wind speed data are sourced from Bureau of Meteorology (BOM— http://www.bom.gov.au/climate/). Average of satellite derived (SeaWiFS via GIOVANNI— https://giovanni.gsfc.nasa.gov/giovanni/) chlorophyll-a data spanned from 1997 to 2010 and in situ chlorophyll data from Pelican Island (AIMS— http://data.aims.gov.au/metadataviewer/uuid/8a698de1-3fbf-48a5-b068-358b07aad35c) and Calliope River mouth (Currie and Small, 2005) spanned from 2007 to 2015 and 1995 to 2001, respectively. Tide height (at Auckland Point, Gladstone— https://www.msq.qld.gov.au/Tides/Open-data) and dissolved phosphate concentration (at

Clinton Wharf, Gladstone—Currie and Small (2005)) data ranged from 2011 to 2014 and 1998 to 2001. Error bars represent standard errors.

Data Statement

Sr/Ca and Ba/Ca data for RI2 and RI1 cores are presented as Data Table 1 and 2 at the end of supporting file.

Highlights

- In contrast to previous findings, *Cyphastrea*'s Ba/Ca does not record changing terrestrial runoff.
- Seasonal cyclicity of Ba/Ca shows summer minima and winter maxima.
- Geochemical cycling of Ba/Ca is influenced by phytoplankton dynamics.
- Geographic and oceanographic conditions are critical for interpreting Ba/Ca signals in coral.

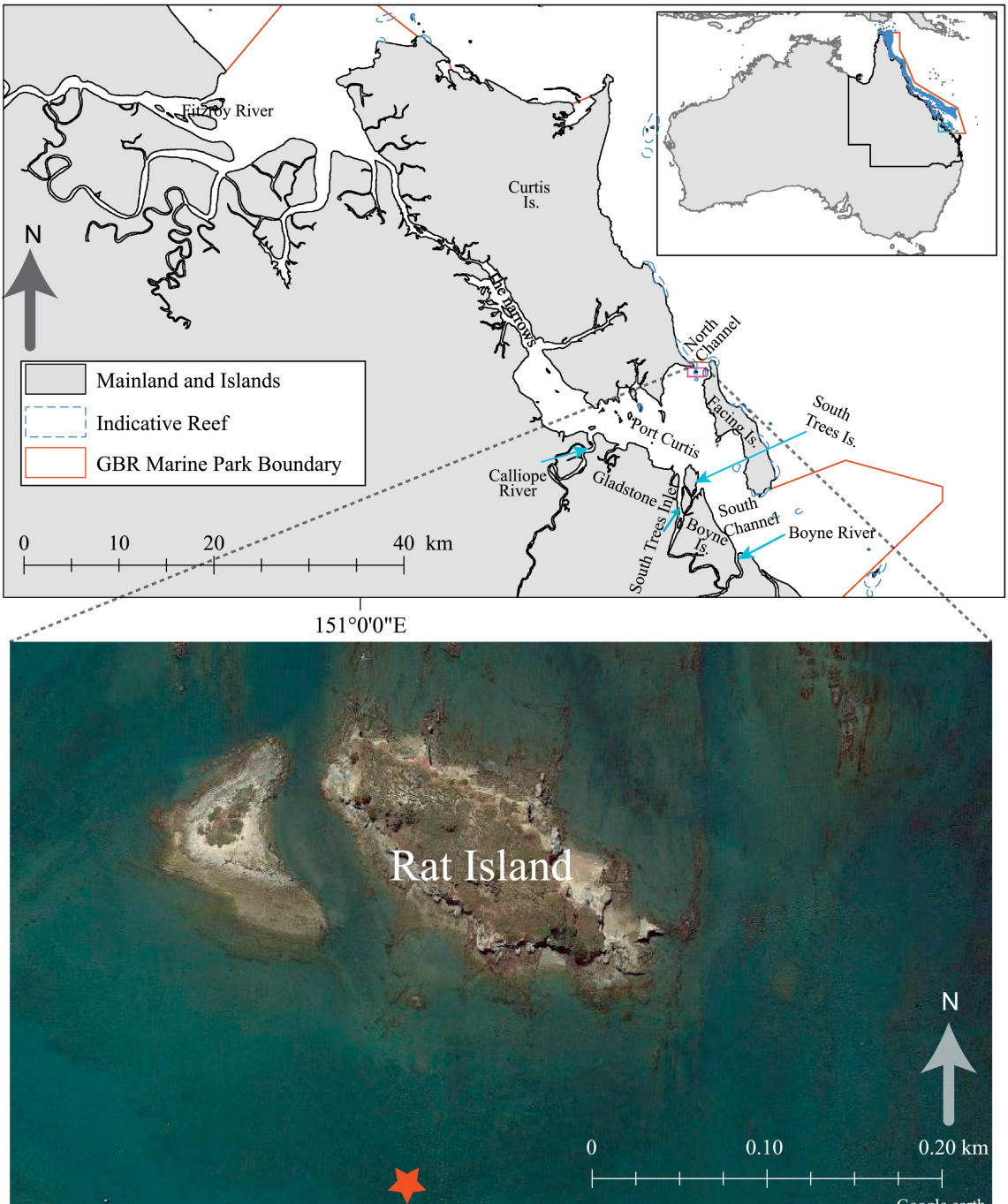
Fitzroy River
Curtis Is.
The Narrows
North Channel
Facing Is.
South Trees Is.
Port Curtis
Calliope River
Gladstone Inlet
South Channel
Boyne Is.
Boyne River
South Trees Inlet
N
Mainland and Islands
Indicative Reef
GBR Marine Park Boundary
0
10
20
40 km
151°0'0"E
Rat Island
N
0
0.10
0.20 km
Google earth

Figure 1

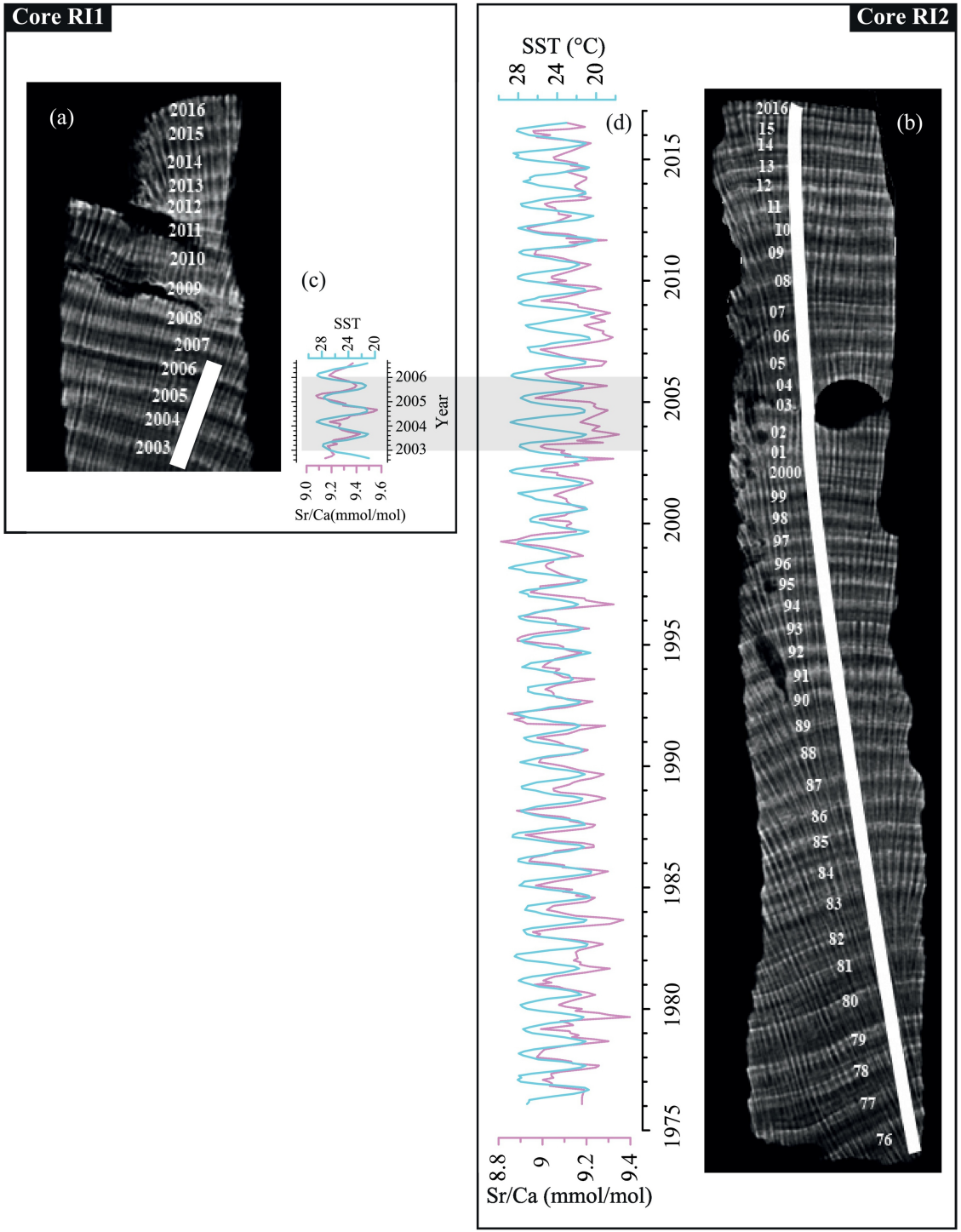
Core RI1
(a)
2016
2015
2014
2013
2012
2011
2010
2009
2008
2007
2006
2005
2004
2003
(c)
SST
28
24
20
2006
2005
2004
2003
Year
9.0
9.2
9.4
9.6
Sr/Ca(mmol/mol)
Core RI2
SST (°C)
28
24
20
(d)
2015
2010
2005
2000
1995
1990
1985
1980
1975
8.8
9
9.2
9.4
Sr/Ca (mmol/mol)
(b)
2016
15
14
13
12
11
10
09
08
07
06
05
04
03
02
01
2000
99
98
97
96
95
94
93
92
91
90
89
88
87
86
85
84
83
82
81
80
79
78
77
76

Figure 2

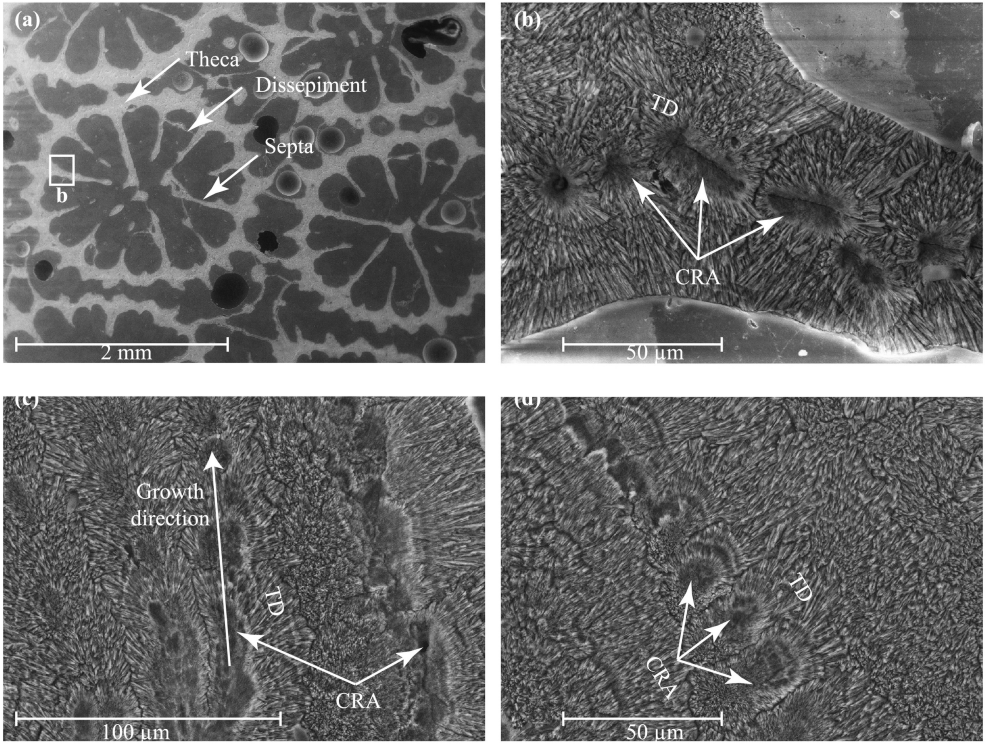
(a)
Theca
Dissepiment
Septa
b
2 mm
(b)
TD
CRA
50 µm
(c)
Growth direction
TD
CRA
100 µm
(d)
TD
CRA
50 µm

Figure 3

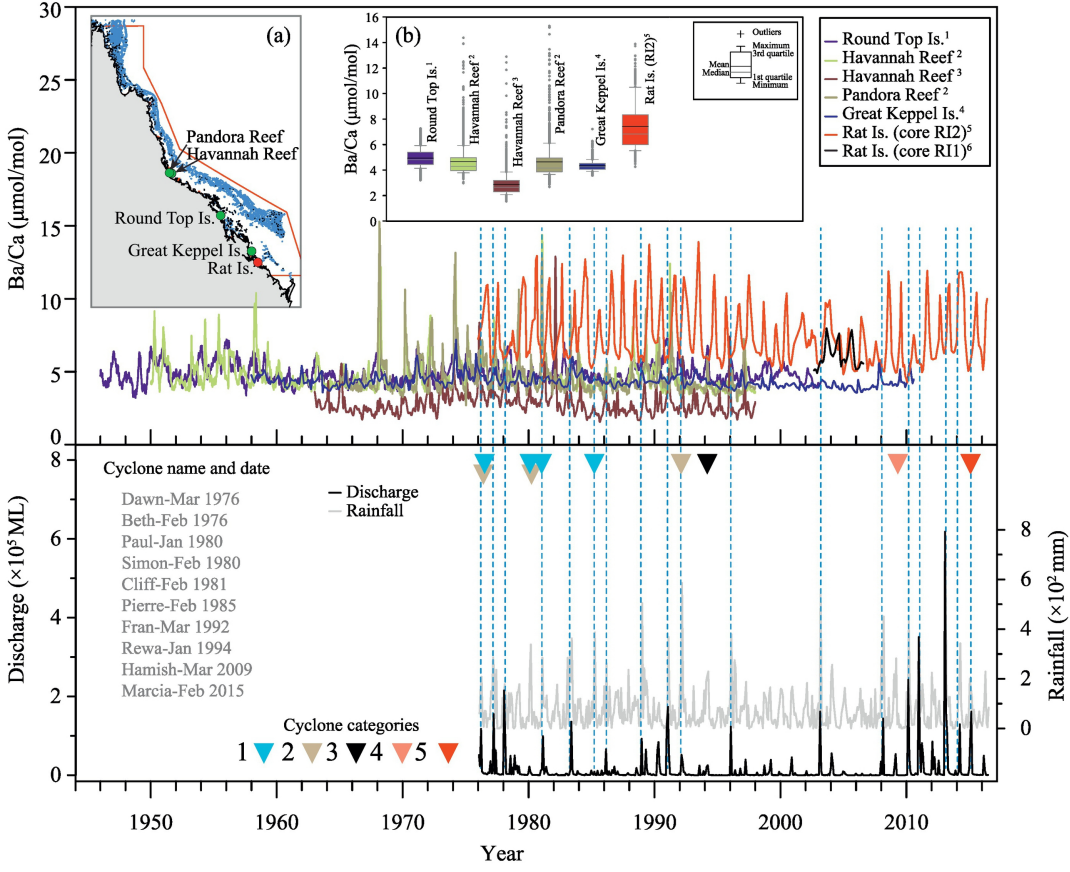
(a)
Pandora Reef
Havannah Reef
Round Top Is.
Great Keppel Is.
Rat Is.
(b)
Ba/Ca (μmol/mol)
Round Top Is.1
Havannah Reef 2
Havannah Reef3
Pandora Reef 2
Great Keppel Is.4
Rat Is. (RI2)5
Outliers
Maximum
3rd quartile
Mean
Median
1st quartile
Minimum
Round Top Is.1
Havannah Reef 2
Havannah Reef 3
Pandora Reef 2
Great Keppel Is.4
Rat Is. (core RI2)5
Rat Is. (core RI1)6
Ba/Ca (μmol/mol)
Cyclone name and date
Dawn-Mar 1976
Beth-Feb 1976
Paul-Jan 1980
Simon-Feb 1980
Cliff-Feb 1981
Pierre-Feb 1985
Fran-Mar 1992
Rewa-Jan 1994
Hamish-Mar 2009
Marcia-Feb 2015
Discharge
Rainfall
Cyclone categories
1 2 3 4 5
Discharge (×10⁵ ML)
Rainfall (×10² mm)
Year

Figure 4

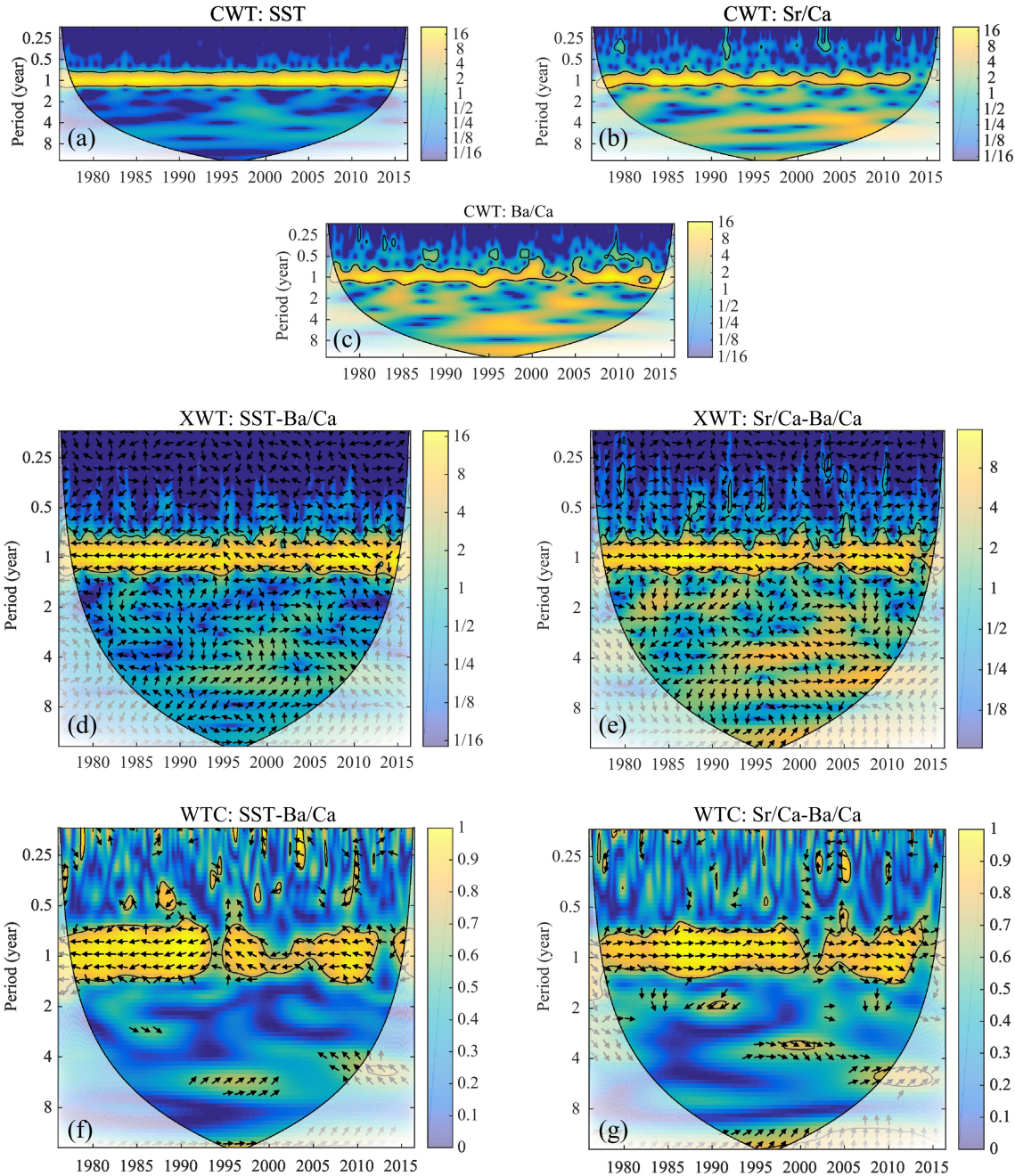
CWT: SST
CWT: Sr/Ca
CWT: Ba/Ca
XWT: SST-Ba/Ca
XWT: Sr/Ca-Ba/Ca
WTC: SST-Ba/Ca
WTC: Sr/Ca-Ba/Ca
Period (year)
0.25
0.5
1
2
4
8
16
1/2
1/4
1/8
1/16
(a)
(b)
(c)
(d)
(e)
(f)
(g)
1980 1985 1990 1995 2000 2005 2010 2015
0.9
0.8
0.7
0.6
0.5
0.4
0.3
0.2
0.1
0

Figure 5

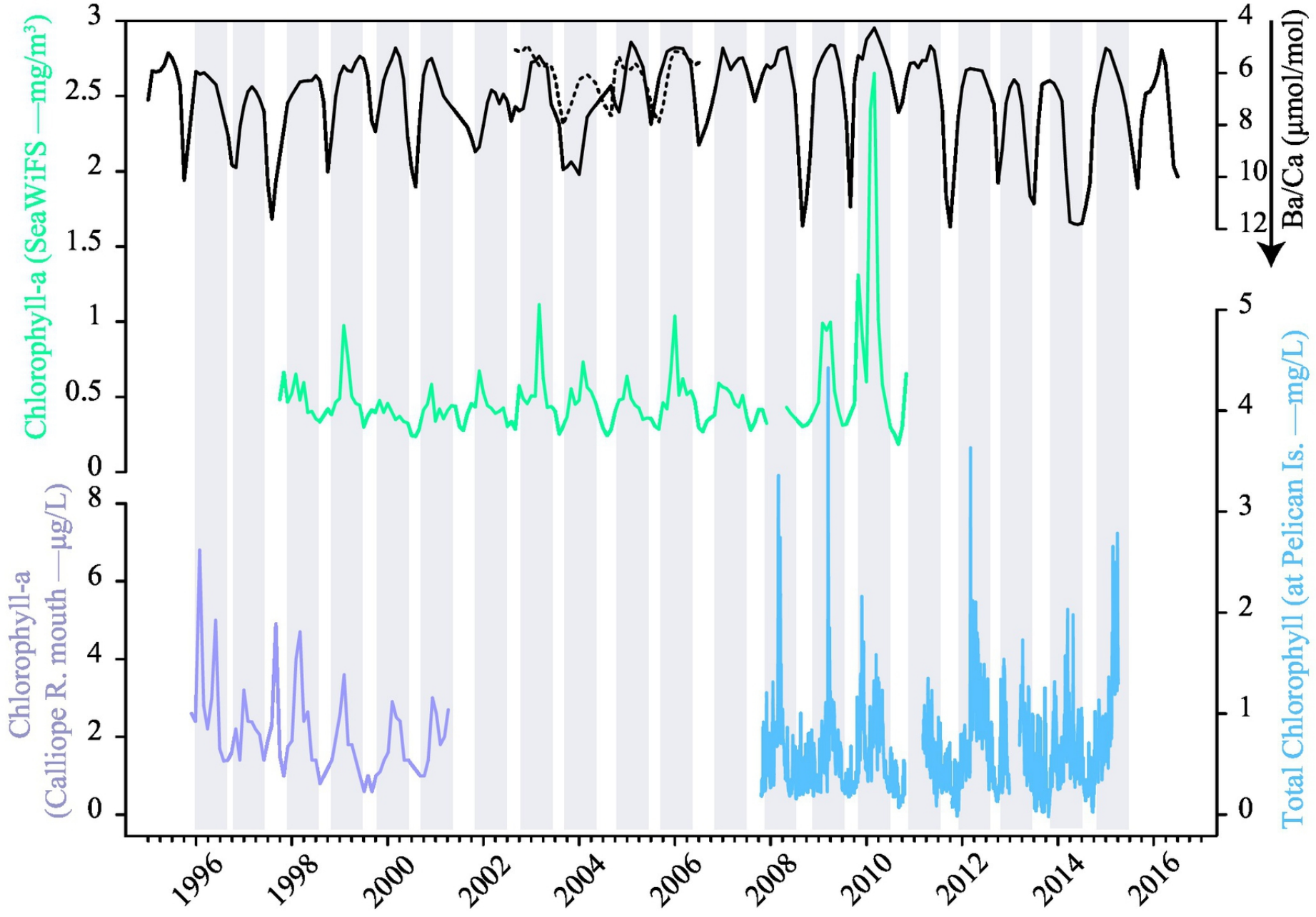
Chlorophyll-a (SeaWiFS —mg/m³)
Ba/Ca (µmol/mol)
Chlorophyll-a (Calliope R. mouth —µg/L)
Total Chlorophyll (at Pelican Is. —mg/L)
3
2.5
2
1.5
1
0.5
0
4
6
8
10
12
5
4
3
2
1
0
8
6
4
2
0
1996
1998
2000
2002
2004
2006
2008
2010
2012
2014
2016

Figure 6

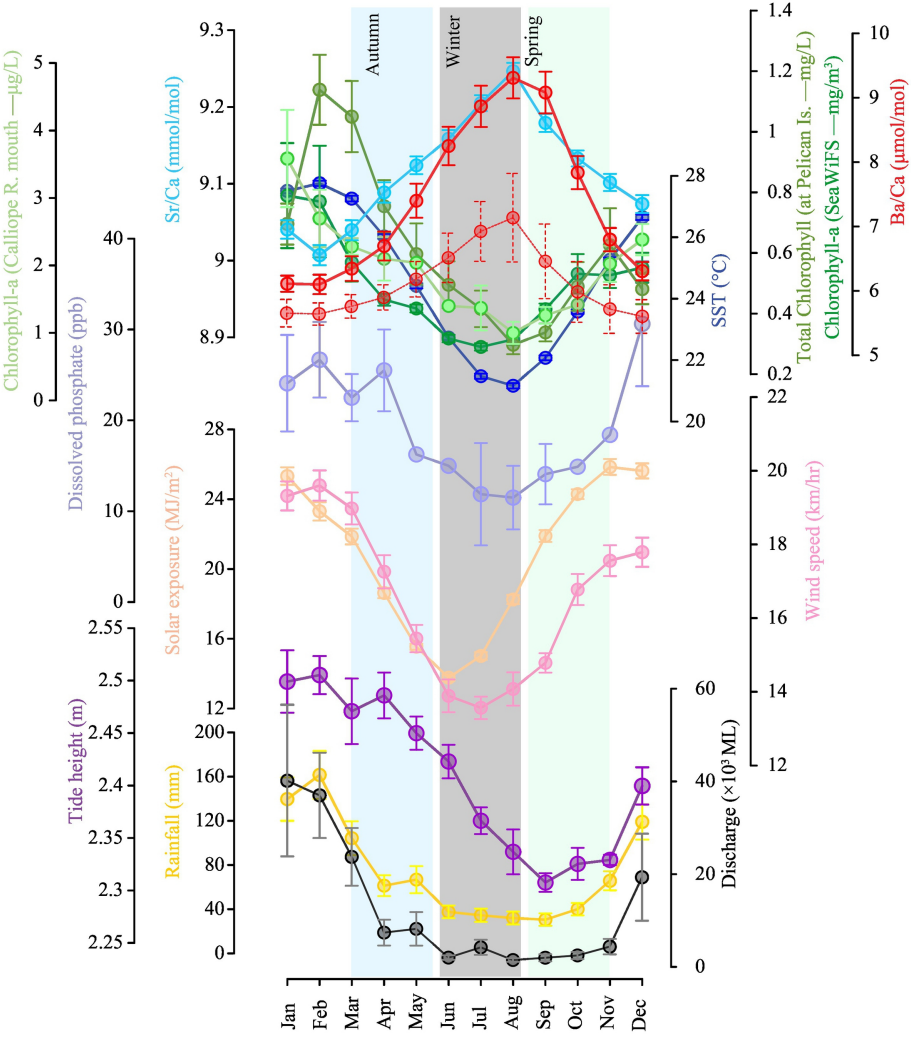
Chlorophyll-a (Calliope R. mouth —µg/L)
Dissolved phosphate (ppb)
Tide height (m)
Rainfall (mm)
Sr/Ca (mmol/mol)
Solar exposure (MJ/m²)
Autumn
Winter
Spring
SST (°C)
Total Chlorophyll (at Pelican Is. —mg/L)
Chlorophyll-a (SeaWiFS —mg/m³)
Ba/Ca (µmol/mol)
Wind speed (km/hr)
Discharge (×10³ ML)
Jan
Feb
Mar
Apr
May
Jun
Jul
Aug
Sep
Oct
Nov
Dec

Figure 7